AMERICAN METEOROLOGICAL SOCIETY

Journal of Climate

EARLY ONLINE RELEASE

The DOI for this manuscript is doi: 10.1175/JCLI-D-12-00539.1

Dynamical Downscaling Projections of 21st Century Atlantic Hurricane Activity: CMIP3 and CMIP5 Model-based Scenarios

Thomas R. Knutson[1], Joseph J. Sirutis[1], Gabriel A. Vecchi[1], Steven Garner[1], Ming Zhao[1], Hyeong-Seog Kim[2], Morris Bender[1], Robert E. Tuleya[3], Isaac M. Held[1], and Gabriele Villarini[4]

[1]Geophysical Fluid Dynamics Laboratory/NOAA, Princeton, NJ 08542

[2]Program in Atmospheric and Oceanic Sciences, Princeton University, Princeton, NJ 08542

[3]Center for Coastal Physical Oceanography, Old Dominion University, Norfolk, VA 23508

[4] IIHR-Hydroscience & Engineering, The University of Iowa, Iowa City, IA

Revised Feb. 8, 2013

Submitted to *Journal of Climate*

Email contact: Tom.Knutson@noaa.gov

Abstract.

Twenty-first century projections of Atlantic climate change are downscaled to explore the robustness of potential changes in hurricane activity. Multi-model ensembles using the CMIP3/A1B (Late 21st century) and CMIP5/RCP4.5 (Early and Late 21st century) scenarios are examined. Ten individual CMIP3 models are downscaled to assess the spread of results among the CMIP3 (but not the CMIP5) models. Downscaling simulations are compared for 18-km grid regional and 50-km grid global models. Storm cases from the regional model are further downscaled into the GFDL hurricane model (9 km inner-grid spacing, with ocean coupling) to simulate intense hurricanes at finer resolution.

A significant reduction in tropical storm frequency is projected for the CMIP3 (-27%), CMIP5-Early (-20%) and CMIP5-Late (-23%) ensembles, and for five of ten individual CMIP3 models. Lifetime-maximum hurricane intensity increases significantly in the high-resolution experiments--by 4 to 6% for CMIP3 and CMIP5 ensembles. A significant increase (+87%) in the frequency of very intense (Category 4-5) hurricanes (winds >= 59 m s^{-1}) is projected using CMIP3, but smaller, only marginally significant increases are projected (+45% and +39%) for the CMIP5-Early and CMIP5-Late scenarios. Hurricane rainfall rates increase robustly for the CMIP3 and CMIP5 scenarios. For the late 21st century, this increase amounts to +20 to +30% in the model hurricane's inner core, with a smaller increase (~10%) for averaging radii of 200 km or larger. The fractional increase in precipitation at large radii (200-400 km) approximates that expected from environmental water vapor content scaling, while increases for the inner core exceed this level.

1. Introduction

The influence of global warming, as projected for the 21st century by current climate models, on hurricane activity in the Atlantic basin is an important research question. Climate model projections from the Coupled Model Intercomparison Project 3 (CMIP3; Meehl *et al*. 2007) and Project 5 (CMIP5; Taylor *et al*. 2012) suggest substantial (~1.5^{o} C) increases over the century in sea surface temperatures (SSTs) in the basin, while wind shear and other storm-influencing factors are projected to change as well (e.g., Vecchi and Soden 2007a,b). Therefore a question arises as to the net impact of these various environmental influences on hurricane activity.

A related issue that arises in attempts to use statistical models to address this problem is the role of local tropical Atlantic SST vs relative SST (that is, tropical Atlantic SST relative to the tropical mean SST) in changing Atlantic hurricane activity. Some statistical relationships linking Atlantic hurricane activity and local tropical Atlantic SSTs suggest a substantial (~2^{o}C) warming of the tropical Atlantic would lead to a large increase (+300%) in a seasonally integrated tropical cyclone power dissipation index (PDI; Emanuel 2005, 2007) (Emanuel 2007; Vecchi *et al*. 2008). Other statistical and dynamical models and physical considerations (e.g., Latif *et al*. 2007; Vecchi and Soden 2007a; Swanson 2008; Bender *et al*. 2010; Zhao *et al.* 2010; Ramsay and Sobel 2011; Vecchi *et al*. 2008, 2011, 2013b; Villarini *et al.* 2011; Villarini and Vecchi 2012a; Camargo *et al*. 2013) suggest that the relative Atlantic SST is a more robust statistical indicator of Atlantic hurricane activity change for the types of climate perturbations relevant for both interannual variability and 21st century climate change projections than is local Atlantic SST. These alternative models suggest relatively much smaller (+/-60%) changes in

65 Atlantic power dissipation over the coming century (Vecchi *et al*. 2008; Villarini and Vecchi
66 2013).

67 Recently, Villarini and Vecchi (2013) provided an updated statistical model projection
68 based on the CMIP5 climate model projections. These new projections include an increase in
69 Atlantic PDI across all 17 CMIP5 models and three representative concentration pathways
70 (RCPs). Since the number of North Atlantic tropical cyclones is not projected to increase
71 significantly in their analysis (Villarini and Vecchi 2012b), they attribute the increased PDI to an
72 intensification of Atlantic tropical cyclones in response to both greenhouse gas (GHG) increases
73 and aerosol changes over the coming decades, with a significant enhancement by non-GHG
74 (primarily aerosol) forcing in the first half of the 21st century.

75 In previous papers (Knutson *et al.* 2007; Knutson *et al.* 2008; Bender *et al.* 2010), we
76 have explored these issues using dynamical downscaling approaches. The present study is an
77 extension of these studies, comparing projections using CMIP5 climate models to the earlier
78 CMIP3 projections. We now include more analysis of the robustness of the CMIP3 projections
79 (Knutson *et al*. 2008; Bender *et al.* 2010) by downscaling ten individual CMIP3 models to
80 explore the spread of projections among the individual models. For the CMIP5 multi-model
81 ensemble projections, we consider both early 21st century and late 21st century projections in
82 light of the findings of Villarini and Vecchi (2013). Individual CMIP5 models have not been
83 examined in our experiments to date.

84 We use three different dynamical downscaling models in different combinations to derive
85 our tropical cyclone projections. The first is a regional 18-km grid atmospheric model (Zetac;
86 Knutson *et al*. 2007) nested within the National Centers for Environmental Prediction (NCEP)

Reanalyses (Kalnay *et al.* 1996). We explore climate change scenarios with this model by perturbing the reanalysis input with climate model-projected changes in large-scale circulation, temperatures, moisture, and SSTs for the late 21st century (Knutson *et al.* 2008). In the second approach, we examine changes in Atlantic tropical storms and hurricanes (up to Category 2) for the same climate change scenarios but use a 50 km grid global atmospheric model (HiRAM; Zhao *et al*. 2009) for the downscaling. For the third approach, we downscale all of the tropical storms and hurricanes from our 18-km grid regional model, on a case-by-case basis, into the Geophysical Fluid Dynamics Laboratory (GFDL) coupled ocean-atmosphere hurricane prediction system (Bender *et al*. 2010) in order to simulate hurricanes with intensities up to Category 4 and 5 intensity. This requires higher model resolution than in the Zetac model to better resolve the storm inner core.

Through these modeling studies we can explore the sensitivity of our projections to different sources of uncertainty. For example, there is uncertainty in the large-scale projected climate changes that are input to the downscaling (i.e., CMIP3 vs CMIP5 multi-model ensemble projections, or the range of projections among individual CMIP3 models). There is also uncertainty in the downscaling results for a given climate change scenario based on the particular model or method used for the downscaling (i.e., the Zetac regional model vs. the HiRAM 50-km grid global model, or the GFDL hurricane model vs. statistical downscaling).

2. Model Description

The models we use at various stages of our hurricane downscaling are summarized in Table 1. These include: a regional atmospheric model for seasonal Atlantic simulations; a

hurricane prediction model for a further downscaling of the individual storms in the regional atmospheric model; and several global climate models, which provide projected late 21st century climate change boundary conditions for our climate change perturbation runs. We also compare our tropical cyclone downscaling results with those from a global atmospheric model run for multi-year "time slices" of the present and projected future climate. The various CMIP3 and CMIP5 climate models and scenarios used in our study are listed in Vecchi and Soden (2007b) and Table 2, respectively, and will be described in more detail later in this section. We assess the significance of our downscaling results using statistical significance tests for both individual model results and for experiments with multi-model ensemble climate change perturbations. These statistical tests assess the strength of the climate change signal in storm behavior relative to the model-derived internal variability (or "weather noise") in our experiments. However, this "weather noise" is just one aspect of the overall uncertainty: a key test of the robustness is the comparison of results between CMIP3 and CMIP5 multi-model ensembles, or between different individual CMIP3 models. These comparisons assess the robustness of our results to the use of different climate models, which is probably a much greater source of uncertainty in the projections than the "weather noise" uncertainty for a single given model. The different downscaling approaches provide another means of assessing robustness of the projections.

a. Zetac Regional Atlantic basin model

For our present climate (control) condition, we simulate 27 seasons (1980-2006; Aug. – Oct. season) of Atlantic hurricane activity using an 18-km grid regional atmospheric model designed specifically to simulate Atlantic hurricane seasonal activity (Knutson *et al*. 2007). This non-hydrostatic model is run without a sub-grid-scale moist convection parameterization (CP), as

discussed below and in Knutson *et al*. (2007). The model is forced at the lower boundary by observed SSTs and at the horizontal boundaries by NCEP Reanalyses, as described in Knutson *et al*. (2007, 2008). This model uses interior spectral nudging (on domain zonal and meridional wavenumbers 0-3, with a nudging timescale of 12 h) to maintain the model's large-scale time-evolving solution close to the NCEP Reanalysis throughout the atmosphere. The same nudging time scale is used for all seasons and experiments (control and global warming cases).

Our philosophy in using interior spectral nudging on large spatial scales only, while not using CP at all, is aimed at maintaining a realistic broad-scale thermodynamic state in the model while allowing resolved convection and condensation in the model to do the work on smaller scales to produce storm genesis. In our view, CP can potentially harm the genesis process. (There are some indications of this in previous studies, such as Han and Pan 2006; Gentry and Lackmann 2006; Zhao *et al*. 2012). Also many aspects of CP remain uncertain, so that our attempt at allowing only model-resolved convective/condensation processes to produce the storm genesis deemed appropriate. Further, the realistic interannual variability obtained with the nudged model is encouraging, particularly since we believe it is important for a model to simulate the relative occurrence of both active and inactive years reasonably well in the control simulation to form an appropriate starting point for a climate change experiment. Global models use CP in part to maintain a realistic mean profile, but at least in the regional model context we can utilize this alternative nudging approach. Due to computational constraints, we have not explored the sensitivity of our Zetac model global warming results to the nudging. We are aware (Zhao *et al*. 2012) that TC simulations in models are sensitive to details such as CP and divergence damping.

For the climate change perturbation runs, the NCEP Reanalysis (i.e., the nudging target) is modified by a seasonally varying climatological change field that includes the projected changes in SST, atmospheric temperature, moisture, and winds from either the CMIP3 or CMIP5 climate models. A discussion of the methods for computing Global Climate Model (GCM) anomalies is given in Section 2d. The atmospheric trace gas (e.g., CO_2, O_3) and aerosol concentrations are not perturbed in the Zetac regional model experiments. However, the influence of these forcings is implicitly incorporated into the model through the three-dimensional climate change field--which is used as boundary conditions and as a nudging target for the interior of the atmospheric domain.

The methodology for identifying tropical storms in the Zetac simulations is described in Knutson *et al*. (2007). Our previous analyses (e.g., Fig. 1 in Knutson *et al*. (2008)) have indicated that the Zetac model reproduces the observed interannual variability of Atlantic hurricane counts over 1980-2006 quite successfully, with a correlation coefficient of 0.84 for modeled vs. observed time series, although the linear trend was about 40% larger than the observed trend. Since our previous study was completed, we have subsequently extended these simulation experiments through 2008. The additional two years substantially over-predict Atlantic hurricane counts (which leads to a linear trend that is about a factor of two larger than observed, and the correlation is reduced to 0.69). We speculate that the less realistic trend in these simulations with the inclusion of the most recent years is derived from large (and presumed spurious) negative trends in NCEP reanalysis temperatures, from the upper troposphere to about 100 hPa (Vecchi *et al*. 2013a). Owing to our concerns about the trend component, it is useful to examine other aspects of the interannual variability. For example, if we remove the linear trend from both modeled and observed hurricane counts, the correlation between the two detrended

177 time series is 0.63 for 1980-2008 or 0.81 for the shorter period (1980-2006). This indicates that
178 the model simulates the non-trend component of variability fairly well, although with poorer
179 agreement for the latest years of 2007 and 2008. Further details on the Zetac model runs and
180 their use in these experiments are provided in Knutson *et al*. (2007, 2008).

181 For the climate change runs, the same interannual variability is present as for the control
182 run, since we add an August-October mean climate change perturbation, which does not change
183 from year to year, onto the NCEP Reanalyses that are used as the nudging target and boundary
184 conditions. This procedure keeps unchanged the large-scale interannual to multi-decadal
185 variations in the interior as well as the high-frequency weather variability imposed at the model
186 boundaries. The method avoids some difficulties in the direct use of climate model simulations,
187 which have known biases (e.g., typically a failure to produce intense hurricanes or realistic
188 hurricane eyewall structure due to their coarse resolution) that can distort tropical storm
189 simulations. It further assumes that the atmospheric variability in the large (interior) scales and
190 the boundary conditions of our control simulation are also representative of variability conditions
191 under the global warming scenario. For example, the occurrence frequency and amplitude of
192 individual El Niño/Southern Oscillation (ENSO) events is unchanged from the observed (1980-
193 2006) in our climate change runs.

194

195 *b. GFDL Hurricane Model*

196 Two versions of the GFDL hurricane model are used to re-simulate at higher resolution
197 the individual storm cases in this study. These model versions are the same as used in Bender *et*
198 *al*. (2010) and include the version used operationally from 2006 through 2012 both at the U.S.

National Weather Service (NWS, 2006-2009; termed the "GFDL Hurricane Model") and the version that has been used by the U.S. Navy (termed the "GFDN Hurricane Model"). In terms of specific differences between the two model versions, the GFDN version allows short-wave radiation penetration into the ocean, has a reduced enthalpy exchange coefficient that is in better agreement with observations, includes a minor bug-fix in the coupler interpolator, and has a minor change in the randomized component of the CP scheme. These changes were not implemented in the NWS version since that model was operationally frozen for several years.

The hurricane model is a triply nested moveable mesh regional atmospheric model coupled to the three-dimensional Princeton Ocean Model (Bender *et al*. 2007). The 5^o latitude by 5^o longitude inner nest of the atmospheric model has a horizontal grid spacing of about 9 km, and is automatically relocated to follow the moving tropical cyclone of interest. The ocean coupling provides an important physical process for the simulations, as it allows the tropical cyclone to interact with the ocean and generate a cold wake in the SSTs which can in turn affect the cyclone's intensity. We used the 18-model average three-dimensional ocean structure change from the CMIP3 models to represent the change in ocean temperature stratification in the warmer climate for all of the hurricane model climate change experiments. Preliminary sensitivity experiments (not shown) indicated that the hurricane model results are relatively insensitive to the details of projected changes in the ocean subsurface temperature profile. (See also Knutson *et al*. 2001.)

Each individual tropical storm and hurricane case from the Zetac regional model was downscaled using the two versions of the hurricane model discussed above. We first identified the time of maximum intensity of the storm in the Zetac model, and then backed up three days from that point to begin the five-day hurricane model integration. This approach tends to

222 preclude looking at integrated storm statistics such as PDI in the hurricane model, since only part
223 of the storm lifetime is simulated. Similarly, landfalling statistics are also not well-captured. We
224 plan to conduct longer (15-day) integrations of the hurricane model in future studies, if possible,
225 to address some of these issues.
226
227 *c. HiRAM C180 global model*

228 To explore the dependence of the tropical storm and hurricane frequency change
229 projections on the model used for downscaling, we compare the Zetac 18-km grid regional
230 model projections to those from a 50-km grid global atmospheric model. The global model
231 (termed HiRAM C180) is described in Zhao *et al*. (2009) along with the method of identifying
232 tropical storms in the model simulations. As shown in Zhao *et al*. (2009), the model realistically
233 simulates the interannual variability of Atlantic hurricane frequency when forced by observed
234 SSTs alone. Other aspects of the simulations from this atmospheric model, such as the simulated
235 mean climate, are described in Held *et al.* (manuscript in preparation). Here, the control run is
236 based on ten repeating seasonal cycles using the observed climatology of SST and sea ice. The
237 climate warming experiments with the model again include ten repeating seasonal cycles, but use
238 the observed climatology modified by changes to SST and sea ice concentration fields. For the
239 CMIP3 experiments, the changes are based on linear trends (2001-2100) from an ensemble of
240 GCMs (Meehl *et al*. 2007) scaled to an 80-year equivalent amplitude (see Section 2d). The
241 forcing change consists of an increase in CO_2 to 720 ppm, with no changes to other climate
242 forcing agents such as aerosols. In the warm-climate runs, the non-negligible effect of an
243 increase in CO_2 in isolation, with prescribed SSTs, (roughly a 20% reduction in both Atlantic
244 tropical cyclones and hurricanes) is described in Held and Zhao (2011).

A second multi-model ensemble forcing experiment was performed using the CMIP5 models. For the CMIP5 runs with the HiRAM model, all greenhouse gases are modified according to the 4.5 W m^{-2} Representative Concentration Pathway (RCP4.5) scenario. Since both the CMIP3 and CMIP5 sets of model experiments are based on ten-year samples (control and late 21st century) using a repeating season cycle, the runs do not include interannual variations such as ENSO. This procedure differs from the procedure used for the Zetac regional model climate change runs (section 2a).

d. Global climate model projections

We use large-scale climate-change projections from global climate models as boundary conditions in these downscaling studies. For the HiRAM C180 global model experiments, we use only the change in SST and sea ice concentrations from the global climate models (which are computed separately for each month of the seasonal cycle), as well as an increase in CO_2 (CMIP3 runs) or all greenhouse gases (CMIP5 runs). For the Zetac regional model late 21st century experiments, we use changes in SST, sea level pressure (SLP), air temperature, relative humidity, and wind velocity to modify the NCEP Reanalysis fields that are used as boundary forcing and as the nudging target for the interior spectral nudging procedure (Section 2a).

For our CMIP3-based experiments with both Zetac and HiRAM-C180, we use either an ensemble average of 18 different CMIP3 models, or individual CMIP3 models. For this study, we tested ten of the 18 individual models. For the ten individual CMIP3 models, we performed the Zetac model downscaling for only the 13 odd years (1981-2005) in order to save computing resources.

The ten selected individual CMIP3 models were chosen from among the 12 highest-ranking models according to a multi-variate performance index for 20th century historical forcing runs (Reichler and Kim 2008). Two of the 12 highest-ranking models were not included in our set due to issues with the archived humidity data that are required for our experiments. We did not attempt to test all 18 models for this study due to computational and time limitations. The ten individual CMIP3 models are shown in Fig. 1. The 18 models comprising the multi-model ensemble are listed in Vecchi and Soden (2007a). For the 18-model ensemble, we used the Aug.-Oct. time average of the years 2081-2100 minus the Aug.-Oct. time average for 2001-2020 (SRES A1B scenario) as the time-invariant, three-dimensional climate change perturbation. When using individual models, we first computed the linear trend through the model fields for 2001-2100, project the model data onto these linear trends, and then compute the difference 2081-2100 minus 2001-2020 of the linear trend projection of the fields as the climate change perturbation. This procedure helps to reduce the contamination of the model climate change signal by the models' internal variability (Knutson *et al*. 2008).

For our CMIP5 experiments, we use data from a second 18-model ensemble based on the RCP4.5 scenario (Table 2). Because of differing data requirements for Zetac and HiRAM, and because of limited availability of sea ice concentration data, we were limited to exploring a 13-model ensemble average with HiRAM, while with Zetac we were able to explore the full 18-model ensemble average. For the CMIP5 models, anomalies were computed as the difference between either the period 2016-2035 or 2081-2100 of the RCP4.5 scenario and the baseline years of 1986-2005 from the historical climate simulations (which is an earlier baseline period, and hence a longer period between averaging periods, than we used for CMIP3). The global surface temperature difference for our climate change perturbation is quite similar for our CMIP3 and

CMIP5 runs (1.69^{o} C vs. 1.70^{o} C, respectively). Our modified approach for CMIP5 allows us to more readily explore projected changes from present climate conditions to either the early (2016-2035) or late (2081-2100) 21st century. This approach was adopted since earlier work (Villarini and Vecchi 2012b, 2013) suggested that the projected TC changes may not evolve linearly over the 21st century. We have not yet performed the downscaling procedure on individual climate models from the CMIP5 archive due to computational and time limitations for the present study.

3. Results

a. Storm Frequency changes

1) CMIP3 DOWNSCALING EXPERIMENTS

The robustness of 21st century model projections of tropical storm and hurricane frequency changes from either the Zetac 18-km grid regional model (a-c) or the GFDL hurricane model (d-h) is explored in Fig. 1. By comparing the results for different models or the CMIP3 vs. CMIP5 multi-model ensembles, and through statistical significance testing of these results, the robustness of our findings can be better assessed. Results are grouped by intensity class of storm, with the weakest storms included in the top panels of the figure (which show all storm of at least tropical storm intensity, or maximum surface winds of at least 17 m s^{-1}) and the most intense storms shown in the bottom panel of the figure.

A striking feature of Fig. 1 is the preponderance of negative changes in the occurrence (i.e., reduced frequency) of weaker storms in the warmer climate, which then shifts

311 systematically to a preponderance of positive changes (increased frequency) for the strongest
312 storms (e.g., Category 4-5 storms with winds of at least 59 m s^{-1} or strong Category 4+ storms
313 with winds exceeding 65 m s^{-1}). This shift is much more apparent for the hurricane model results
314 (d-h) than for the Zetac regional model (a-c) which does not simulate high-intensity (Category 4
315 and 5) storms.

316 Tables 3 and 4 summarize these projected changes for the various classes of storms.
317 Table 3 shows results for the 18-model CMIP3 ensemble based on 27-year samples, whereas
318 Table 4 focuses on results for individual CMIP3 models and examines only the 13 odd years in
319 the sample. While CMIP3 multi-model ensemble results for the 13 odd years are shown in Table
320 4 for completeness, the multi-model ensemble results in Table 3 are emphasized here since they
321 include a larger sample (all 27 seasons or years). For the CMIP3 18-model ensemble-mean
322 climate change projection, the Zetac regional model simulates a significant (p-value <0.01) 27%
323 reduction in tropical storm frequency (Table 3). The range across ten individual CMIP3 models
324 was -62% to +8% (Table 4), with five of ten individual models showing a significant (p-
325 value<0.05) decrease. The average of the ten individual models (not shown) is a decrease of
326 30%, or comparable to the simulated decrease (-33%) for the 13 odd years using the 18-model
327 average climate change perturbation.

328 For hurricane frequency in the Zetac model, the 18-model ensemble CMIP3 change is -
329 17% (Table 3), though not statistically significant (p-value equal to 0.15). The range across the
330 ten individual CMIP3 models for hurricane frequency (Table 4) is -66% to +22% with three of
331 ten models showing a significant (p<0.05) decrease. There is little significant change (Fig. 1) in
332 major hurricanes in the Zetac model (Category 3-5 hurricanes, based on a central pressure
333 criterion of less than 965 hPa).

For the more intense classes of hurricanes, we focus on dynamical downscaling results from the GFDL hurricane model (ensemble of GFDL and GFDN model versions), as shown in Fig. 1 (f-h). The hurricane models' frequency projections for major hurricanes (Category 3-5) are summarized as follows: no significant change (-17%) for the 18-model ensemble climate change (Table 3), with a significant decrease (increase) for four (two) of ten individual CMIP3 models (Table 4). The average change for the ten individual CMIP3 models (-13%, not shown) is not significant, and the range across the individual models is -88% to +71%.

For Category 4-5 storms, a significant increase in frequency (+87% with a p-value of 0.01) is simulated for the warmer climate using the 18-model ensemble mean CMIP3 model climate change, as was shown in Bender *et al*. (2010). For the ten individual models (Table 4), the range of Category 4-5 frequency changes is -100% to +210%, with three of the ten model downscalings showing a significant (p-value <0.05) increase.

Strong Category 4+ hurricanes with winds exceeding 65 m s^{-1} occur about once per decade in the control run compared with about once every two years in the observations (Table 3). The frequency of these storms increases significantly (+250%; p-value of 0.05) for the 18-model ensemble mean CMIP3 climate change. The change for the average of the ten individual CMIP3 models is +90% but not statistically significant (not shown). The ten individual models (Table 4) show a range of changes of -100% to +480%, with three of ten individual models showing a significant increase. The Atlantic basin PDI shows a strong tendency for decreases in the Zetac model (Tables 3, 4), as expected based on the basin-wide changes in the various hurricane categories. While the projected changes in U.S. landfalling tropical storm and hurricane counts tend to be negative in the individual CMIP3 model experiments, the decreases in the CMIP3 ensemble mean climate change scenario were not statistically significant.

As an alternative to the second dynamical downscaling step using the hurricane model, we also applied a statistical refinement for hurricane intensity directly to the Zetac regional model data (Zhao and Held 2010). This statistical refinement is based on matching the percentiles of the model's control run distribution to the observed wind speed distribution, which substantially lowers the wind speed threshold used to identify higher-category hurricanes in the model. The results using this alternative approach (Table 3) show a similar overall behavior to that from dynamical downscaling using the GFDL hurricane model – at least for the frequency of weak storms. However, a statistically less robust increase in the frequency of stronger storms is projected using the statistical refinement approach, compared to dynamical downscaling (Table 3).

The downscaling projections for the frequency of Atlantic tropical storms and hurricanes for the CMIP3 and CMIP5 ensemble mean climate change and individual CMIP3 models can also be compared between the Zetac regional model and the GFDL HiRAM C180 global climate model (Fig. 2). The scatterplot comparison in Fig.2 was done for the subset of CMIP3 models that is common to the experiments done with these two downscaling models. The HiRAM C180 model (50-km grid) uses prescribed SST changes from the CMIP models. In contrast, the Zetac model is additionally forced by atmospheric temperature, wind, and moisture changes; these are internally generated by the C180 model. The 18-model ensemble and seven of the ten individual models were in common among the downscaling experiments currently available using these two downscaling models.

For tropical storms, in the C180 experiments, all seven individual CMIP3 models and the 18-model ensemble climate change show reduced frequency, compared to the Zetac experiments, where six of seven individual models and the 18-model ensemble show a decrease. The

correlation between the seven individual CMIP3 model percent change results is 0.77. For hurricanes, five of seven individual CMIP3 models and the 18-model ensemble yield a decrease in frequency using C180, while four of seven individual models plus the 18-model ensemble show a decrease in frequency for Zetac. If we look for consistency of hurricane downscaling response for individual CMIP3 models, only one of the seven models shows an increase in hurricane frequency in both the C180 and Zetac downscaling experiments (upper right quadrant) while three show a decrease in both (lower left quadrant). Still the correlation among the individual model percent change values is 0.73 for the hurricane changes.

2) CMIP5 VS. CMIP3 RESULTS

As a test of the robustness of our results to the use of the new CMIP5 climate models, we have downscaled an 18-model ensemble climate change scenario obtained from the CMIP5 models (early and late 21st century projections). We have not yet had the opportunity to examine individual climate model downscalings for the CMIP5 models. The ensemble results for storm frequency are summarized and compared graphically in Figs. 1 and 2, and summarized in tabular form in Table 3. Fig. 1 shows that the basic result from CMIP3 of a significant decrease in the frequency of tropical storms and hurricanes, is robustly reproduced using the independent CMIP5 climate change scenarios (early and late 21st century). In terms of quantitative comparison (Table 3), the tropical storm frequency change from the Zetac regional model is -27% for CMIP3 compared with -23% for CMIP5-Late (see also Fig. 2). The reduction is almost as large for CMIP5-Early (-20%). For hurricane (Category 1-5) frequency, the Zetac regional model shows nominal decreases of -17% (p-value equal to 0.15) for CMIP3 and -19% (p-value equal to 0.08) for CMIP5-Late) indicating marginal significance for the latter case. For U.S.

403 landfalling tropical storms (hurricanes), the projected change is -17% (-23%) for CMIP3 and
404 +3% (-12%) for CMIP5-Late, but none of these changes are statistically significant. For the PDI,
405 the 18-model ensemble results show significant decreases of -17% (p-value equal to 0.04) for
406 CMIP3 and -20% (p-value of 0.03) for CMIP5-Late, which may be relatively more significant
407 owing to the aggregated nature of the metric.

408 Concerning the frequency of the more intense hurricanes, we can compare the hurricane
409 model downscaling results for CMIP3 and CMIP5 scenarios in Table 3 and Fig. 1. The
410 frequency changes have a tendency to shift from negative (for tropical storms) to positive (for
411 very intense hurricanes) for both the CMIP3 and CMIP5-Early and CMIP5-Late ensembles,
412 although the statistical significance of the positive changes for intense hurricanes for CMIP5 is
413 not as robust as for the CMIP3. For example, for Category 4-5 hurricanes the frequency increase
414 (+87%) was significant (p-value of 0.01) for CMIP3, while for CMIP5-Early and CMIP5-Late,
415 the changes were still positive (+45% and +39%) but not quite significant at the 5% level (p-
416 values of 0.06 and 0.11, respectively, according to the Mann-Whitney-Wilcoxon test). Using a t-
417 test (not shown in Table 3) results in a slightly more significant assessment of the changes (p-
418 value of 0.04 for CMIP3; p-value of 0.05 for CMIP5-Early and p-value of 0.08 for CMIP5-Late).
419 In summary, the projected increases in Category 4-5 frequency are significant for the
420 CMIP3/A1B scenario, but are only marginally significant for the CMIP5-Early climate change
421 scenario and even less significant for the CMIP5-Late scenario.

422 For very intense hurricanes with winds of at least 65 m s^{-1}, we find similar results to
423 Category 4-5, with large (+250%) and significant (p-value equal to 0.05) increases for the
424 CMIP3/A1B scenario, but with only nominally positive changes in frequency for CMIP5 (+83%
425 for both CMIP5-Early and CMIP5-Late; Table 3). Neither of the CMIP5-based increases is

426 statistically significant (p-values of 0.25 and 0.17). U.S. landfalling statistics are not presented
427 for the stronger systems owing to the fact that the higher (Category 4-5) storms are only
428 simulated explicitly with the GFDL hurricane model. Those runs, which by design are limited to
429 5-day duration beginning 3 days prior to maximum intensity in the host (Zetac) model, are not
430 well-suited for examination of U.S. landfall frequency. In fact, landfall often did not occur
431 within the 5-day timeframe of the storm experiment even in cases where a landfall eventually did
432 occur in the (host) Zetac model. For these reasons, the U.S. landfalling hurricane and tropical
433 storm frequency changes obtained using the hurricane model downscaling framework (Table 3)
434 should be treated with caution.
435
436 *b) Storm intensity changes*

437 1) CMIP3 INTENSITY RESULTS

438 The changes to hurricane characteristics with climate warming can also be examined in
439 terms of frequency histograms of lifetime-maximum wind speeds (one value per storm) as shown
440 in Figs. 3, 4 and Tables 3, 4 for the CMIP3 downscaling. The Zetac model histograms in Fig. 3
441 show the clear deficiency of the Zetac model (present day "Control" simulation) at reproducing
442 the observed intensity distribution (black dashed line), particularly for higher intensities; the
443 Zetac model also simulates too many moderate intensity storms. These shortcomings have
444 largely motivated our use of the GFDL hurricane model for this study. The higher resolution
445 hurricane model simulates a more realistic distribution of storm intensities than Zetac,
446 particularly above 50 m s^{-1} (Fig. 4), although it remains deficient at simulating the observed
447 frequency of the highest intensity storms (Table 3).

There is considerable spread in the climate change experiment results among the different individual CMIP3 models as shown in Figs. 3 and 4, yet it is possible to see the common tendency of fewer storms overall in the warm climate runs than in the control runs. While this reduction holds at most intensities, the tendency reverses to one of greater occurrence of storms at the high intensity end in the warmer climate--at least for most of the individual models. This amounts to a change in the shape of the normalized histogram for both the Zetac model (Fig. 3c, d) and the GFDL hurricane model (Fig. 4), such that the normalized distribution becomes slightly flatter and more spread out. The consistency of the response of the higher intensity storms is easier to discern in Fig. 1, which focused on the frequency of particular categories of storms, thus allowing for a particular focus on the higher-intensity storms. Such intense storms are relatively rare in observations compared to the typical hurricanes, and so they tend to be de-emphasized in intensity histograms that depict the entire intensity distribution (e.g., Figs. 3 and 4). They nonetheless have important implications for hurricane damage potential. For example, Pielke *et al*. (2008) conclude that Category 4-5 hurricanes were responsible for nearly half of historical U.S. hurricane damage even though they account for only about 15% of U.S. landfalling tropical cyclones.

2) CMIP 5 VS. CMIP3 INTENSITY RESULTS

The ensemble intensity distributions for CMIP3 and CMIP5, shown in Fig. 6, depict a "flattening" and spreading out of the intensity distribution, along with an overall reduction in frequency. That is, the high intensity end of the intensity distribution evolves differently from the middle of the distribution, as is seen by the increase in frequency of strong storms despite the reduction in the frequency of storms for all categories combined. This feature is present for both

471 CMIP3 and CMIP5 (Early and Late 21st century), although it is less apparent for the CMIP5 due
472 to the smaller (only marginally significant) change projected for the frequency of the strongest
473 hurricanes (Table 3).

474 An alternate way of assessing intensity changes is to examine the average of the lifetime
475 maximum intensities for all storms above certain threshold intensities. Table 3 shows that for the
476 hurricane model, the average maximum wind intensity for hurricanes (winds greater than 33 m s^{-1}
477) increases by about 4-6% for the CMIP3 and CMIP5 (Early and Late-21st century) ensembles,
478 and that these changes are statistically significant. Table 4 shows that the range among individual
479 CMIP3 models for this metric is -3% to +12%, with nine of ten models showing at least a
480 nominal increase. For all tropical storms and hurricanes combined, the model ensemble changes
481 are smaller (0.7% to 3.4%) and only significant for the CMIP5-Early. Nonetheless, the mean
482 change in hurricane intensity is very likely more relevant for assessing hurricane damage
483 potential. The changes in mean lifetime maximum intensity for the storms in the Zetac regional
484 model are generally smaller than for the hurricane model (-0.7% to +3.5%) but the Zetac model
485 has pronounced deficiencies at simulating the intensity distribution, and so is considered less
486 suitable for examining this metric, compared to the hurricane model. To attempt to address the
487 low bias of the intensity simulation with the Zetac model, that model's results can be statistically
488 refined (following Zhao and Held 2010) to explore the behavior of higher intensity storms at
489 least statistically. Figure 5 shows a scatterplot of hurricane intensity change results obtained
490 using statistical refinement vs. that using dynamical downscaling. Both approaches show a
491 preponderance of positive changes, although as can been seen in Table 3, the changes obtained
492 using statistical refinement for the multi-model ensemble mean CMIP3 and CMIP5 climate
493 change scenarios tend to be smaller and/or less statistically significant than those from the

494 dynamical downscaling (hurricane model) approach. For the individual CMIP3 models the
495 intensity changes tend to be slightly larger for the statistical refinement approach, as most of the
496 individual model symbols in Fig. 5 lie above the diagonal line.

497 In summary, for the CMIP3 and CMIP5 ensemble mean climate changes, the projected
498 changes of mean intensities have a clear positive tendency, especially for hurricanes in the higher
499 resolution model downscaling experiments. The results for the individual models (Table 4) have
500 a clear tendency for increases, but also have a much wider range among the experiments. For the
501 high resolution (hurricane model) runs only one individual model (HadGEM1) shows a negative
502 change of hurricane intensity; none of the models show a nominally negative change for the
503 Zetac runs. Considering all tropical cyclones, rather than just hurricanes, several individual
504 models show negative intensity changes in the high resolution runs, and two individual models
505 do so in the Zetac experiments. Note that since only half of the seasons (odd years only) were
506 downscaled for the individual model cases it is perhaps not surprising that the signals for the
507 individual models tend to be less robust, owing to the lower expected signal to noise ratio.
508
509 *c) Storm track and occurrence changes*

510 We present here a brief analysis of changes in the geographical distribution of storm
511 tracks. We focus on the Category 4-5 results for the CMIP3 and CMIP5 ensemble climate
512 change experiments using the GFDL hurricane model. Tracks for the GFDL hurricane model for
513 Category 4-5 storms obtained from the GFDL/NWS version are shown on the left column of Fig.
514 7, while those for the GFDN version are shown on the right column; results are compared from
515 the CMIP3 and CMIP5 (Early and Late 21st century) ensemble runs. As noted earlier (Table 3),
516 the increase in frequency of Category 4-5 storms is statistically significant (p-value equal to

517 0.01) for the CMIP3 ensemble but only marginally significant for the CMIP5 ensembles,
518 especially for the Late-21st century CMIP5. Nonetheless, it is of interest to compare the track
519 maps for the Category 4-5 storms for the various scenarios. The comparison of the geographical
520 distribution of storm occurrence is examined in Fig. 8. The occurrence of Category 4-5 storms
521 shows more of a tendency for a shift toward the Gulf of Mexico and Florida region for the
522 CMIP5 climate change runs than for the CMIP3 climate change runs. In the CMIP3 runs, the
523 increase of Category 4-5 storms was more focused over the western Atlantic (i.e., centered
524 further from a number of U.S. landfalling regions).

525 In any case, these differences in regional detail between the CMIP3- and CMIP5-based
526 intense hurricane track projections should be viewed with a caution against over-interpretation of
527 such regional-scale details, despite the strong interest regarding the climate impacts at these
528 scales. For example, we have not yet demonstrated that our model is capable of providing useful
529 climate variability or change information, based on past storm data, at these smaller spatial scales
530 (in contrast to the basin-wide statistics). In addition, our hurricane model experiments are a
531 maximum of five-day duration, and are of limited utility for examining U.S. landfalling storm
532 behavior. We are planning to address this limitation in future studies.

533 The reduction in tropical storm frequency coupled with a tendency for an increase of
534 intense storm occurrence (Figs. 7, 8, and Table 3) can be further explored in terms of large-scale
535 environmental changes simulated by the CMIP3 and CMIP5 models for the SRESA1B (CMIP3)
536 and RCP4.5 (CMIP5) scenarios. Figure 9 shows maps of the projected changes in tropical
537 cyclone potential intensity (PI), vertical wind shear, SST, and local SST relative to the tropical
538 mean SST, as discussed in Vecchi and Soden (2007a). Also shown for comparison are results
539 from 2xCO_2 transient experiments with the CMIP3 and CMIP5 models (which are based on

linear trends from years 1-70 of +1%/yr CO_2 experiments obtained from the CMIP3 and CMIP5 model archives). Each of the CMIP3 and CMIP5 multi-model 21st century scenarios shows a band of minimum (or even negative) PI change across the Atlantic basin. While some areas of PI decrease are simulated, the PI changes are predominantly positive over the basin's main tropical cyclone regions as a whole. The regions of projected PI decrease are smaller and less pronounced in the CMIP5 RCP4.5 runs than in the CMIP3 or 2xCO_2 runs. Similarly, the CMIP3/A1B and the 2xCO_2 runs (for both CMIP3 and CMIP5) show large regions of negative relative SST across the Atlantic, in contrast to the CMIP5/RCP4.5 ensembles. These regions of negative relative SST correspond roughly to regions with enhanced vertical wind shear. Since a decrease in tropical storm frequency was found for the CMIP5/RCP4.5 as well as CMIP3/A1B downscaling, we speculate that the change in the wind shear of the mean circulation is not the primary driver of the decrease in Atlantic tropical storm frequency seen across our experiments. Moreover, the CO_2-only experiments, which show the increased shear and decreased relative SST for both CMIP3 and CMIP5, indicate that the absence of these features in the CMIP5/RCP4.5 ensemble is apparently related to changes in non-greenhouse radiative forcing (RCP4.5 vs. SRES-A1B) as opposed to changes in the models' responses to increasing greenhouse gases (c.f., the similarity of CMIP5 and CMIP3 CO_2-only responses). The preponderance of positive potential intensity changes of a few meters per second in the CMIP3/A1B and CMIP5/RCP4.5 scenarios is broadly consistent with the simulated increase in lifetime maximum intensities of hurricanes in our hurricane model downscaling, and with the increase in frequency of very intense (Category 4-5) hurricanes.

The CMIP3 and CMIP5 (Early and Late-21st century) model projections generally indicate an amplified warming response in the upper troposphere compared to the surface (not

563 shown, but see Knutson and Tuleya (2004) or Hill and Lackmann (2011)). For example, the
564 mean warming at 300 hPa is about 2.2 times larger than near the surface for the Main
565 Development region (MDR; 10^{o}N-20^{o}N; 80^{o}W-20^{o}W) for both the CMIP3 and the CMIP5
566 ensembles; for nine of the ten individual CMIP3 models, the warming ranges from about 1.9 to
567 2.7 times larger than near the surface (with HadGEM1 being an outlier, with a factor of 3.5).
568 These changes are thus broadly similar to those reported in the previous studies. The enhanced
569 warming with height in the climate model projections likely limits the hurricane intensity
570 increase in response to climate warming as simulated in the hurricane model (e.g., Shen et al.
571 2000; Knutson and Tuleya 2004; Emanuel et al. 2013; Vecchi et al. 2013a), compared to what it
572 would be for a hypothetical uniform warming with height, for example.

573 We have computed storm propagation speed statistics from our storm samples (labeled
574 "Trans speed" in Tables 3 and 4). The results for the CMIP3 and CMIP5 ensembles indicate no
575 significant changes, and only two of the ten individual CMIP3 model projections show a
576 significant change (increase). In short, there is not a clear consistent signal in the storm
577 propagation speed projections.

578

579 *d) Storm-related precipitation rate changes*

580 A robust feature in our model projections is an increase of precipitation rates averaged
581 within the near-storm region. Figure 10 (a, b) summarizes the statistical analysis for the average
582 precipitation rate within 100 km of the storm center for all tropical storms and hurricanes
583 combined in the Zetac (a) and hurricane model (b) experiments, including results for the
584 individual CMIP3 models experiments. This metric includes the entire storm lifetime (or up to

five days in the case of the hurricane model runs), which is dominated by the time spent over the open ocean. Thus, the precipitation results shown here primarily represent hurricane-related rainfall over the ocean, as opposed to landfalling or inland storms. For the Zetac model, the average change for the CMIP3 18-model ensemble is +19%, while for the CMIP5-Early and CMIP5-Late ensembles the average change is +8% and +13%, respectively (Table 3), with all changes being statistically significant. In the hurricane model (Fig. 10b, Table 3), the changes are even larger, with an increase of +22% for the CMIP3 ensemble, +18% for CMIP5-Early and +19% for CMIP5-Late. For the ten individual CMIP3 models that we have examined, Table 4 shows that in the Zetac model runs, all ten runs have a positive change in this metric, ranging from +11% to +28%, with nine out of ten having statistically significant increases (p-value<0.05) according to the Mann-Whitney-Wilcoxon test. For the hurricane model downscaling runs, seven of ten individual models have significant increases in the 100-km averaged precipitation rate. Tables 3 and 4 show that the precipitation-rate projections for hurricanes are similar to those for all tropical storms and hurricanes combined; however, they are less robust statistically, especially in the Zetac model runs. For example, only five of ten individual models show a significant increase in this metric for Zetac, while seven of ten have a significant increase in the hurricane model runs. The changes for the CMIP5-Early ensemble are consistently much smaller than for the CMIP5-Late ensemble for the Zetac model, but this distinction is not as evident for the hurricane model runs. The results hint that the precipitation rate changes (Fig. 10 and Table 3) are more closely tied to absolute temperature changes than hurricane frequency changes are. The precipitation-rate results show a consistent positive tendency across a number of model projections for both downscaling models, whereas the hurricane frequency changes tend to be negative for hurricanes up to Category 3 but positive for Categories 4 and 5. Previous

608 studies that have explored this metric have generally found that an increase in tropical cyclone
609 precipitation rates is a relatively robust climate change response (see review in Knutson *et al*.
610 (2010)).

611 Figure 10 (c) shows a model-by-model scatterplot comparison of precipitation rate
612 change results for the Zetac vs hurricane model downscaling runs. The comparison shows a
613 relatively good agreement between the two downscaling methods in their projections of changes
614 in precipitation rate, although the hurricane model tends to project a larger percentage increase in
615 future precipitation rate than does the (lower resolution) Zetac model.

616 Figure 11 shows the precipitation rate changes for CMIP3 and CMIP5-Late ensembles,
617 for both the Zetac and hurricane models, as a function of averaging radius about the storm center,
618 varying from 50 km to 400 km. For all sets of experiments, the percentage increase is amplified
619 nearer to the storm, but then tends to an asymptote to roughly +10% at larger radii (~200-400
620 km). We can use a simple moisture scaling argument to interpret the asymptotic behavior at
621 larger radii. If we assume that the moisture budget within the broad near-storm environment
622 (within 400 km of the center) is dominated by moisture convergence from the larger
623 environment, then fractional increases in atmospheric moisture content in the warmer
624 atmosphere should lead to similar fractional increases in the moisture convergence and thus in
625 precipitation rate. A representative SST change for our experiments (Aug.-Oct. mean, averaged
626 10-25^{o}N, 20-80^{o}W) is 1.7^{o}C for CMIP3 and 1.3^{o}C for CMIP5-Late. Assuming a 7% increase in
627 lower tropospheric atmospheric water vapor content per degree Celsius SST change, we obtain
628 the ~10% increases depicted by the dashed lines in Fig. 11 for the CMIP3 and CMIP5
629 environments. Thus our results show that this scaling argument describes our model
630 precipitation increases fairly well for averaging radii of 200-400 km. However, the more

631 amplified model precipitation response at smaller radii (between 50 km and 150 km) does not
632 agree with this simple scaling. The amplification of the fractional increase near the storm center
633 is most pronounced in the higher resolution hurricane model runs, where increases of the order of
634 20% and 33% occur at averaging radii of 100 and 50 km. For the Zetac model, the increases are
635 of the order of 15% (25%) for radii of 100 (50) km. These results suggest that other processes,
636 such as intensification of the hurricane circulation, may play a more important role in the
637 response of the hurricane inner-core precipitation rates to climate warming.

638

639 **4. Discussion and Conclusions**

640 In this study, we have conducted a large number of numerical experiments to explore the
641 dependence of Atlantic hurricane activity on projected climate changes as obtained from the
642 CMIP3 and CMIP5 coupled model data archive. We have compared downscaling results for
643 CMIP3 against CMIP5-Early- and CMIP5-Late-21st century projections, and examined the
644 spread of the results within a ten-member subset of the 18 individual models used to form the
645 CMIP3 ensemble.

646 We have used two different downscaling models--an 18-km grid regional model (Zetac)
647 and a 50-km grid global model (HiRAM C180)--and have simulated substantial sets (27) of
648 three-month seasons or years of hurricane activity in order to examine the robustness of the
649 initial downscaling step. We focus especially on the simulated frequency of tropical storms and
650 hurricanes, as the interannual variability of these metrics since 1980 is well-produced by these
651 models (e.g., Knutson *et al*. 2008; Zhao *et al.* 2009). A caveat to the Zetac model results is that
652 the overall frequency of simulated tropical storms in the model is sensitive to the nudging

timescale used, as shown in Knutson *et al*. (2007). In order to study the most intense hurricanes, we have performed an additional downscaling step on the individual storms in the Zetac model, using two versions of a 9-km grid operational hurricane prediction model with ocean coupling. This hurricane model has been developed and refined for operational hurricane prediction use, and thus it can simulate more intense systems and more realistic spatial structures for hurricanes than the lower resolution downscaling models.

Several findings with varying degrees of robustness have emerged from this study. One of the most striking features from the Zetac regional model is its consistent projection of *fewer* Atlantic tropical storms in warmer climates. The ensemble model changes are -27% (CMIP3), -20% (CMIP5-Early), and -23% (CMIP5-Late), and all statistically significant. The range across individual CMIP3 models is -62% to +8%, with five of ten models showing a statistically significant decrease. Our results quoted above from the Zetac regional model are overall rather similar to those from the C180 global model (Fig. 3). On the other hand, as shown in a recent review (Knutson *et al*. 2010), agreement on the sign of the projected change of Atlantic tropical storm frequency results is not as robust when one considers other published studies. Examples of studies which project at least nominally positive changes in Atlantic tropical storm frequency include Sugi *et al*. (2002), Oouchi *et al*. (2006), Chauvin *et al.* (2006; one of two models), Emanuel *et al.* (2008), Sugi *et al.* (2009; six of eight experiments), and Murakami *et al.* (2011; one of three multi-model ensemble experiments). Further insight on the differences in model projections can be gained by re-plotting the tropical storm frequency projections of several published studies in a scatterplot (Fig. 12) against the statistical downscaling projection of Villarini *et al*. (2011). The Villarini *et al.* projected changes are approximately proportional to the change in relative SST for the MDR. The comparison shows that dynamical models

projecting increased tropical storm frequency were usually forced with (or had computed within the model) SST warming in the tropical Atlantic that exceeded the tropical-mean warming. The variance explained by the statistical downscaling model is 55%. Thus the analysis helps to reconcile the differences between the different published Atlantic tropical storm projections and our current results.

A second robust result is an increase in the mean lifetime maximum intensity of hurricanes. In terms of storm frequencies for various categories, the projections typically show a reduction in the overall frequency storms and hurricanes, but with an increase in the frequency of the most intense hurricanes. The transition from decreasing to increasing storm frequency, as one moves to higher intensity classes, is one of the most robust intensity-related features in our hurricane model simulations. This transition is seen most clearly in the figures examining changes in the frequency of different categories of storms (Fig. 1), but is also apparent in the histograms of storm intensities for the hurricane model (Figs. 4, 6). The feature is more pronounced in the hurricane model than in the Zetac regional model (Fig. 1). We have emphasized the hurricane model results in our assessment of strong intensities, because that model has a much more realistic simulation of intense hurricanes than the Zetac regional model. The projected increase in Category 4-5 hurricane frequency (+87%) is statistically significant in our experiments for the CMIP3 18-model ensemble climate change and for three of the ten individual CMIP3 models (Fig. 1; Table 4). This feature is also present in the CMIP5 (Early and Late-21st century) downscalings, although there the change is smaller in magnitude (+45% and +39%, respectively) and only marginally significant, particularly for the CMIP5-Late ensemble. A less robust change in intense storm frequencies is derived by using a statistical refinement of the Zetac intensities (Table 3), as opposed to dynamical downscaling using the hurricane model.

699 The related increase in mean lifetime-maximum storm intensity is apparent in the
700 simulations—particularly in the (higher resolution) hurricane model downscaling runs shown in
701 Table 3--and is more pronounced for storms of at least hurricane intensity than for all tropical
702 cyclones with winds exceeding 17 m s^{-1}. In Knutson *et al*. (2010), the globally averaged mean
703 intensity of tropical cyclones was assessed as likely to increase with climate warming, although
704 they noted that the uncertainties of such projections were larger for individual basins. In their
705 Table S2 (Intensity Projections), the published intensity projections for the Atlantic basin
706 showed relatively small changes in some studies, and ranged even to negative values for some
707 individual models that were analyzed (e.g., Vecchi and Soden 2007). In a recent idealized study
708 with regional models of 6- and 2-km grid spacing, Hill and Lackmann (2011) report an intensity
709 increase of 9%-14% for the late 21st century Atlantic conditions in terms of central pressure
710 deficit. Dividing by two for a rough comparison with our wind speed results, Hill and
711 Lackmann's projections would be a 4.5% and 7% increase for the 6- and 2-km model. Our
712 current results for hurricane intensities (a statistically significant +4% to +6% increase for the
713 CMIP3 and CMIP5-Early and Late multi-model ensemble conditions, with a range of -3% to
714 +11% for individual CMIP3 models) are generally consistent with these earlier findings.
715 Individual model downscaling for this metric tend to show a larger range than the multi-model
716 ensemble downscalings (and are based on a smaller sample of years in our study), although even
717 those results show a clear preference for an increase.

718 While very intense hurricanes are relatively rare, their importance is considerable. For
719 example, Mendelsohn *et al*. (2012) note: "With the present climate, almost 93% of tropical
720 cyclone damage is caused by only 10% of the storms." Of even greater relevance to our results
721 is an analysis of U.S. hurricane damage statistics partitioned by storm category (Pielke *et al*.

722 2008). They conclude that Category 4-5 hurricanes were responsible for nearly half of historical
723 U.S. hurricane damage even though they account for only about 15% of U.S. landfalling tropical
724 cyclones. Clearly, the strongest tropical cyclones inflict a disproportionate impact on society in
725 terms of storm damage.

726 A final robust feature of our simulations is the increase in storm-related precipitation
727 rates, which is significant in the CMIP3 and CMIP5 (Early and Late 21st century) ensemble
728 results and for most of the individual CMIP3 models examined. The fractional rate of increase is
729 amplified for averaging radii less than about 150 km (Fig. 11). Our results show that the
730 hurricane precipitation rate increases robustly in the warm climate simulations in both the Zetac
731 regional model and the GFDL hurricane model. The near-storm amplification is larger in the
732 hurricane model than in the Zetac regional model. Increases of order 20% (33%) occur at
733 averaging radii of 100 (50) km, respectively for the hurricane model. At relatively larger
734 averaging radii (roughly 200-400 km), the model results appear to asymptote to change levels
735 close to what would be expected from simple Clausius-Clapeyron atmospheric water vapor
736 scaling arguments. Our precipitation results are broadly consistent with and provide further
737 support for results in a recent review of tropical cyclone climate change simulation studies
738 (Knutson *et al*. 2010) and with the recent Atlantic hurricane downscaling study of Hill and
739 Lackmann (2011).

740 A notable difference relative to our previously published work (Bender *et al*. 2010) is that
741 the CMIP5/RCP4.5 ensemble climate change projections (Early- and Late-21st century), when
742 downscaled, lead to only marginally significant (+45% and +39%) increases in the frequency of
743 Category 4-5 hurricanes. In contrast, the CMIP3/A1B ensemble leads to a larger (+87%)
744 statistically significant increase in Category 4-5 hurricanes. Our results for high intensity storms

745 can also be compared with those of Murakami *et al*. (2012), who used a high-resolution global
746 model but reported Category 5 storm results also for the Atlantic basin for a late 21st century
747 CMIP3/A1B ensemble scenario (auxiliary information provided by Dr. H. Murakami, personal
748 communication, 2011). Their model projects a non-significant increase in Category 4-5 storm
749 days in the Atlantic basin (+15%) and globally (+4%). For Category 5 storm days, their model
750 projects significant increases (+56% globally, and +290% in the Atlantic basin). There are
751 several important caveats to the results from the various models. For example, the GFDL
752 hurricane model has a substantial (~50%) low bias in its simulation of Atlantic Category 4-5
753 hurricane frequency under present climate conditions (1980-2006). Murakami *et al*. report a
754 relatively small bias in their present-day simulation of Atlantic Category 5 storm days, but a
755 large positive bias (almost a factor of 4) in their simulation of Atlantic Category 4-5 storm days.
756 In addition, the global model used by Murakami *et al*. does not include an interactive ocean
757 component, in contrast to the hurricane model used in the present study and Bender *et al.* (2010).

758 The underestimation of Category 4-5 storm frequency in our hurricane model simulations
759 compared to observations (Table 3) is a limitation of our modeling system in the context of this
760 paper and Bender *et al*. (2010). However, we are not aware of any other dynamical modeling
761 study to date that produces a more realistic simulation of Atlantic Category 4-5 frequency,
762 including the multi-decadal variation of storm intensity (Bender *et al* 2010, their Fig. 1 a-d). Our
763 judgment is that the intensity distribution in our model is realistic enough at the Category 4-5
764 level that we can start to take the frequency projections of these very intense storms seriously.
765 We have chosen to present changes in Category 4-5 storm numbers in terms of fractional
766 changes rather than absolute changes because of the bias in our control simulations. It is our
767 judgment that this is an appropriate way to attempt to account for the bias at the present time. A

768 more satisfying remedy awaits improvements in our model (e.g., increase of resolution to better
769 resolve the storm core and eyewall region (Chen *et al*. 2007; Gentry and Lackmann 2010) which
770 we hope will lead to a simulated frequency of Category 4-5 storms that is closer to the observed.

771 The question arises whether the projected increases in Category 4-5 storm frequency
772 would be detectable in the 21st century if they occurred. Bender *et al*. (2010) estimated that the
773 CMIP3/A1B increase of about 10% per decade would require roughly six decades to be
774 detectable as a linear trend. The projected change for CMIP5-Early of a 45% increase for 2016-
775 2035 compared to 1986-2005 is another possible candidate signal for detection. The difficulty is
776 in estimating the internal variability noise in which this signal would be embedded. In an
777 idealized assumption, we can try to estimate the noise from examination of the Category 4-5
778 observations (see supplemental material of Bender *et al*. (2010)). If the internal variability is
779 estimated from either the raw observations or as the residual from a linear trend through the
780 observed data, then the projected change (45%) would not be significant. However, if we
781 assume that the forced signal in Category 4-5 hurricanes is a fourth-order polynomial fit through
782 the original observed time series, and the residual from this fourth-order fit is the internal
783 variability, then the projected CMIP5-Early signal would be detectable above the internal
784 variability noise. In short, this idealized analysis suggests that whether the increase in Category
785 4-5 frequency we project for the CMIP5 scenario will detectable or not depends on the estimate
786 of internal variability noise, which remains uncertain at this time.

787 Considering hurricanes with winds exceeding 65 m s^{-1} (which occur about once per
788 decade in the control run compared with about once every two years in the observations), the 18-
789 model ensemble mean CMIP3 change from the hurricane model is statistically significant
790 (+250%), compared to smaller (non-significant) changes of +83% for both CMIP5-Early and

791 CMIP5-Late models. Of the ten individual CMIP3 models, three showed a significant increase.
792 Note that the low bias in such storms (about 20% of the observed rate) is even more severe than
793 the ~50% low bias for Category 4-5 storms as discussed above. As mentioned above, future
794 plans include possibly re-doing these experiments with a higher resolution version of our
795 hurricane model (6 km inner mesh) that is currently under development, in order to improve the
796 control simulations of these extreme events. In addition, the statistical significance of some of
797 our results might be enhanced through longer simulations even for the present models.

798 Overall, our results provide further support to previous studies projecting that
799 anthropogenic warming in the Atlantic basin over the 21st century will lead to fewer tropical
800 storms and hurricanes overall, but that the mean intensity of Atlantic hurricanes basin-wide will
801 increase. The projected increase in the frequency of very intense (Category 4-5) hurricanes is
802 statistically significant for the CMIP3 ensemble climate change, but only marginally significant
803 for the CMIP5 Early and Late-21st century ensembles. A robust signal is that tropical storms and
804 hurricanes in the warmer climate are projected to have substantially higher rainfall rates than
805 those in the current climate. The projected hurricane precipitation rate increase by the late 21st
806 century scales roughly with the fractional increase in total precipitable water vapor content
807 (~+11%), particularly at relatively larger radii (200-400 km), but shows even larger fractional
808 increases (order +20% to 30%) near the hurricane core.

809

810 **Acknowledgments.** We thank Ron Stouffer and Lucas Harris of GFDL, Kerry Emanuel of MIT,
811 and two anonymous reviewers for helpful comments on our work. We acknowledge PCMDI and
812 the modeling groups contributing to the CMIP3 and CMIP5 model archives for generously

making their model output available to the community. Funding support from the Willis Research Network for Hyeong-Seog Kim and Gabriele Villarini is gratefully acknowledged. We thank Isaac Ginis and Richard Yablonsky of the Univ. of Rhode Island for assistance with the hurricane model ocean coupling components.

References

Bender, M.A., I. Ginis, R.E. Tuleya, B. Thomas, and T. Marchok, 2007: The operational GFDL coupled hurricane-ocean prediction system and a summary of it performance. *Mon Wea. Rev*., **135,** 3965-3989.

Bender, M. A. T. R. Knutson, R. E. Tuleya, J. J. Sirutis, G. A. Vecchi, S. T. Garner, and I. M. Held, 2010: Modeled impact of anthropogenic warming of the frequency of intense Atlantic hurricanes. *Science* **327**, 454–458.

Camargo, S., M. Ting, and Y. Kushnir, 2013: Influence of local and remote SST on North Atlantic tropical cyclone potential intensity, *Clim. Dyn. (submitted).*

Chen, S. S., W. Zhao, M. A. Donelan, J. F. Price, and E. J. Walsh, 2007: The CBLAST-Hurricane Program and the next-generation fully coupled atmosphere-wave-ocean models for hurricane research and prediction. *Bull. Amer. Meteor. Soc.,* **88,** 311-317.

Emanuel, K. 2005: Increasing destructiveness of tropical cyclones over the past 30 years. *Nature,* **436,** 686–688.

Emanuel, K., 2007: Environmental factors affecting tropical cyclone power dissipation. *J. Climate*, **20,** 5497–5509.

Emanuel, K., S. Solomon, D. Folini, S. Davis, and C. Cagnazzo, 2013: Influence of tropical tropopause layer cooling on Atlantic hurricane activity. *J. Climate* (in press).

Emanuel, K., R. Sundararajan, and J. Williams, 2008: Hurricanes and global warming—Results from downscaling IPCC AR4 simulations. *Bull. Amer. Meteor. Soc.,* **89,** 347–367.

839 Gentry, M. S., and G. M. Lackmann, 2006: The Sensitivity of WRF Simulations of Hurricane
840 Ivan to Choice of Cumulus Parameterization. Preprints, 27th Conf. on Hurricanes and
841 Tropical Meteorology, Monterey, CA, Amer. Meteor. Soc., P5.14. [Available online at
842 https://ams.confex.com/ams/pdfpapers/108539.pdf].
843
844 Gentry, M. S., and G. M. Lackmann, 2010: Sensitivity of simulated tropical cyclone structure
845 and intensity to horizontal resolution. *Mon. Wea. Rev.,* **138,** 688-704.
846 IPCC, 2007: *Climate Change 2007: The Physical Science Basis.* Eds. Solomon, S. *et al.*
847 Cambridge Univ. Press.
848 Han, J., and Pan, H.-L., 2006: Sensitivity of hurricane intensity forecast to convective
849 momentum transport parameterization. *Mon. Wea. Rev.,* **134,** 664–674.
850 Hill, K. A., and G. M. Lackmann, 2011: The impact of future climate change on TC intensity
851 and structure: a downscaling approach. *J. Climate*, **24,** 4644-4661. doi:
852 http://dx.doi.org/10.1175/2011JCLI3761.1
853 Kalnay, E., and Coauthors, 1996: The NCEP/NCAR 40-Year Reanalysis Project. *Bull. Amer.*
854 *Meteor. Soc.*, **77,** 437–471.
855 Knutson, T. R., J. McBride, J. Chan, K. A. Emanuel, G. Holland, C. Landsea, I. M. Held, J.
856 Kossin, A. K. Srivastava, and M. Sugi, 2010: Tropical cyclones and climate change. *Nat.*
857 *Geosci.*, **3,** 157-163, doi:doi:10.1038/ngeo779.
858 Knutson, T. R., J. J. Sirutis, S. T. Garner, I. M. Held, and R. E. Tuleya, 2007: Simulation of the
859 recent multidecadal increase of Atlantic hurricane activity using an 18-km-grid regional
860 model. *Bull. Amer. Meteor. Soc.,* **88**(10), doi:10.1175/BAMS-88-10-1549.

861 Knutson, T. R., J. J. Sirutis, S. T. Garner, G. A. Vecchi, and I. M. Held, 2008: Simulated
862 reduction in Atlantic hurricane frequency under twenty-first-century warming conditions.
863 *Nat. Geosci.*, **1**, 359–364, doi:10.1038/ngeo202.
864 Knutson, T. R., and R. E Tuleya, 2004: Impact of CO_2-induced warming on simulated hurricane
865 intensity and precipitation: Sensitivity to the choice of climate model and convective
866 parameterization. *J. Climate*, **17**(18), 3477-3495.
867 Knutson, T. R., R. E. Tuleya, W. Shen, and I. Ginis, 2001: Impact of CO2-induced warming on
868 hurricane intensities simulated in a hurricane model with ocean coupling. *J. Climate,*
869 **14**(11), 2458-2468.
870 Latif, M., N. Keenlyside, and J. Bader, 2007: Tropical sea surface temperature, vertical wind
871 shear, and hurricane development. *Geophys. Res. Lett*., **34,** L01710,
872 doi:10.1029/2006GL027969.
873 Meehl, G. A. *et al*., 2007: The WCRP CMIP3 multimodel dataset: A new era in climate change
874 research. *Bull. Amer. Meteor. Soc.* **88,** 1383–1394.
875 Mendelsohn, R., K. Emanuel, S. Chonabayashi, and L. Bakkensen, 2012: The impact of climate
876 change on global tropical cyclone damage. *Nature Climate Change*, **2,** 205-209.
877 Murakami, H., Y. Wang, H. Yoshimura, R. Mizuta, M. Sugi, E. Shindo, Y. Adachi, S.
878 Yukimoto, M. Hosaka, S. Kusunoki, T. Ose, A. Kitoh, 2012: Future changes in tropical
879 cyclone activity projected by the new high-resolution MRI-AGCM. *J. Climate*, **25,** 3237-
880 3260.
881 Oouchi, K., J. Yoshimura, H. Yoshimura, R. Mizuta, S. Kusumoki, and A. Noda, 2006: Tropical
882 cyclone climatology in a global warming climate as simulated in a 20-km-mesh global

883 atmospheric model: Frequency and wind intensity analysis. J. *Meteor. Soc. Japan,* **84,**
884 259–276.
885 Pielke, R.A., J. Gratz, C.W. Landsea, D. Collins, M.A. Saunders, and R. Musulin, 2008:
886 Normalized hurricane damages in the United States: 1900–2005. *Nat. Hazards Rev*. **9**,
887 29–42.
888 Ramsay, H.A., and A.H. Sobel, 2011: Effects of relative and absolute sea surface temperature on
889 tropical cyclone potential intensity using a single-column model. *J. Climate*, **24**, 183–
890 193.
891 Reichler, T. and J. Kim, 2008: How Well Do Coupled Models Simulate Today's Climate? *Bull.*
892 *Amer. Meteor. Soc.*, **89** (3), 303-311. doi: http://dx.doi.org/10.1175/BAMS-89-3-303.
893 Shen, W., R. E. Tuleya, and I. Ginis, 2000: A sensitivity study of the thermodynamic
894 environment on GFDL model hurricane intensity: Implications for global warming. *J.*
895 *Climate*, **13**, 109–121.
896 Sugi, M., H. Murakami, and J. Yoshimura, 2009: A reduction in global tropical cyclone
897 frequency due to global warming. *SOLA*, **5,** 164–167.
898 Swanson, K.L., 2008: Nonlocality of Atlantic tropical cyclone intensities. *Geochemistry*
899 *Geophysics Geosystems*, 9, Q04V01, doi:10.1029/2007GC001844
900 Taylor, K.E., R.J. Stouffer, and G.A. Meehl, 2012: An overview of CMIP5 and the experiment
901 design. *Bull. Amer. Meteor. Soc.*, **93,** 485-498.
902 Vecchi, G. A. and Soden, B. J., 2007a: Increased tropical Atlantic wind shear in model
903 projections of global warming. *Geophys. Res. Lett.* **34,** L08702.
904 Vecchi, G.A., and B.J. Soden, 2007b: Effect of remote sea surface temperature change on
905 tropical cyclone potential intensity, *Nature*, **450,** 1066-1070 doi:10.1038/nature06423.

906 Vecchi, G. A., K. L. Swanson, and B. J. Soden, 2008: Whither hurricane activity. *Science* **322,**
907 687–689.
908 Vecchi, G.A., M. Zhao, H. Wang, G. Villarini, A. Rosati, A. Kumar, I.M. Held, and R. Gudgel,
909 2011: Statistical-dynamical predictions of seasonal North Atlantic hurricane activity.
910 *Mon. Wea. Rev.*, **139**(4), 1070-1082.

911 Vecchi, G.A., S. Fueglistaler, I.M. Held, T.R. Knutson, M. Zhao, 2013a: Impacts of Atmospheric
912 Temperature Changes on Tropical Cyclone Activity, *J. Climate* (in press).

913 Vecchi, G.A., R. Msadek, W. Anderson, Y. C. Chang, T. Delworth, K. Dixon, R. Gudgel, A.
914 Rosati, B. Stern, , G. Villarini, A. Wittenberg, X. Yiang, R. Zhang, S. Zhang, and F.
915 Zeng, 2013b: Multi-year predictions of North Atlantic hurricane frequency: Promise and
916 limitations, *J. Climate* (in press).

917 Villarini, G., and G.A. Vecchi, 2012a: North Atlantic Power Dissipation Index (PDI) and
918 Accumulated Cyclone Energy (ACE): Statistical modeling and sensitivity to sea surface
919 temperature changes. *J. Climate*, **25**(2), 625-637.

920 Villarini, G., and G.A. Vecchi, 2012b: Twenty-first-century projections of North Atlantic
921 tropical storms from CMIP5 models. *Nature Climate Change*, 2, 604-607.

922 Villarini, G., and G.A. Vecchi, 2013: Projected Increases in North Atlantic Tropical Cyclone
923 Intensity from CMIP5 Models. *J. Climate.* doi: 10.1175/JCLI-D-12-00441.1 (in press)

924 Villarini, G., G.A. Vecchi, T.R. Knutson, M. Zhao, and J.A. Smith, 2011: North Atlantic tropical
925 storm frequency response to anthropogenic forcing: Projections and sources of
926 uncertainty. *J. Climate*, **24**(13), 3224-3238.

927 Zhao, M., and I. M. Held, 2010: An analysis of the effect of global warming on the intensity of
928 Atlantic hurricanes using a GCM with statistical refinement. *J. Climate*, **23**(23),
929 DOI:10.1175/2010JCLI3837.1.

930 Zhao, M., I. M. Held, S.-J. Lin, and G. A. Vecchi, 2009: Simulations of global hurricane
931 climatology, interannual variability, and response to global warming using a 50km
932 resolution GCM. *J. Climate*, **22**(24), DOI:10.1175/2009JCLI3049.1.

933 Zhao, M., I.M. Held, and G. A. Vecchi, 2010: Retrospective forecasts of the hurricane season
934 using a global atmospheric model assuming persistence of SST anomalies. *Mon. Wea.*
935 *Rev.*, **138,** 3858–3868.

936 Zhao, M., I.M. Held, and S.-J. Lin, 2012: Some counter-intuitive dependencies of tropical
937 cyclone frequency on parameters in a GCM. *J. Atmos. Sci.*, **69**(7), DOI:10.1175/JAS-D-
938 11-0238.1.

939

940 **TABLE 1.** Summary of the experiments and models used for both the control (present-day) and
941 21st century experiments.
942

MODEL/Scenario:	CMIP3 Climate Change Scenario	CMIP5 Climate Change Scenario
Regional Climate Model (Zetac); 18 km grid	18-member ensemble mean climate change for SRES A1B, late 21st century (27 season samples); Ten individual CMIP3 models (13-season samples)	18-member ensemble mean climate change for RCP4.5, early and late 21st century samples; (27 season samples)
Storm-following Hurricane Model (GFDL and GFDN versions); 9 km inner grid	All Tropical cyclone cases from the above Zetac runs	All Tropical cyclone cases from the above Zetac runs
GCM: HiRAM (50 km grid)	18-member ensemble mean climate change for A1B, late 21st century (10 repeating seasonal cycles); 7 individual CMIP3 models are in common with the CMIP3 models used with the Zetac model	13-member ensemble mean for RCP4.5 late 21st century (10 repeating seasonal cycles)

943
944

945

946 **TABLE 2.** Summary of the 18 CMIP5 (Taylor *et al*. 2012) GCMs used in this study to create the
947 multi-model anomalies. The last two columns indicate the models for which the required data to
948 create boundary conditions for Zetac (SST, SLP, air temperature, relative humidity, and winds;
949 total 18 models) and HiRAM (SST and sea ice concentration; total 13 models) were available.

Modeling Center (or Group)	**Model Name**	**Used in ZETAC**	**Used in HiRAM**
Canadian Centre for Climate Modelling and Analysis	CanESM2	Y	Y
National Center for Atmospheric Research	CCSM4	Y	
Centre National de Recherches Meteorologiques / Centre Europeen de Recherche et Formation Avancees en Calcul Scientifique	CNRM-CM5	Y	Y
Commonwealth Scientific and Industrial Research Organization in collaboration with Queensland Climate Change Centre of Excellence	CSIRO-Mk3.6.0	Y	Y
	FGOALS-g2	Y	Y
NOAA Geophysical Fluid Dynamics Laboratory	GFDL-CM3	Y	Y
NOAA Geophysical Fluid Dynamics Laboratory	GFDL-ESM2G	Y	Y
NOAA Geophysical Fluid Dynamics Laboratory	GFDL-ESM2M	Y	Y
Met Office Hadley Centre	HadGEM2-CC	Y	
Met Office Hadley Centre	HadGEM2-ES	Y	Y
Institut Pierre-Simon Laplace	IPSL-CM5A-LR	Y	
Institut Pierre-Simon Laplace	IPSL-CM5A-MR	Y	
Atmosphere and Ocean Research Institute (The University of Tokyo), National Institute for Environmental Studies, and Japan Agency for Marine-Earth Science and Technology	MIROC5	Y	Y

Japan Agency for Marine-Earth Science and Technology, Atmosphere and Ocean Research Institute (The University of Tokyo), and National Institute for Environmental Studies	MIROC-ESM	Y	Y
Japan Agency for Marine-Earth Science and Technology, Atmosphere and Ocean Research Institute (The University of Tokyo), and National Institute for Environmental Studies	MIROC-ESM-CHEM	Y	
Max Planck Institute for Meteorology	MPI-ESM-LR	Y	Y
Meteorological Research Institute	MRI-CGCM3	Y	Y
Norwegian Climate Centre	NorESM1-M	Y	Y

950

951

952 Table 3. Storm statistics from CMIP5 vs. CMIP3-based downscaling experiments for Atlantic
953 tropical storms and hurricanes, based on comparing 27 Aug.-Oct. seasons (1980-2006) with and
954 without a climate change perturbation. CMIP3 and CMIP5 refer to storm climate changes
955 simulated using climate change information from the CMIP3/A1B and CMIP5/RCP4.5 multi-
956 model ensembles. "CMIP5-Early" and "CMIP5-Late" perturbations are for years 2016-2035 and
957 2081-2100, respectively, compared to the historical simulations (years 1986-2005). "Control"
958 refers to our present-day downscaling simulations (1980-2006). The hurricane model results are
959 for the average of runs using two model versions (GFDL and GFDN). Frequencies are in
960 number per year (Aug.-Oct. only). "Cat" is Saffir-Simpson intensity Category (1-5) with "Cat 0"
961 signifying less than hurricane strength. "Trans speed" is storm translation speed in m s^{-1}. Rain
962 rate is the average rain rate within 100 km of the storm center in mm day^{-1}. PDI is power
963 dissipation index in units of 10^9 m^3 s^{-2}. "Hur_ws>65" refers to hurricanes with surface wind
964 speeds greater than or equal to 65 m s^{-1}. "Maxwnd_ts" and "maxwnd_hur" are mean lifetime
965 maximum intensities for all tropical storms (wind speed > 17.5 m s^{-1}) or hurricanes (wind speed
966 > 33 m s^{-1}). For the statistical adjustment method, there were no Category 5 hurricanes in the
967 control or for either of the CMIP5 ensembles; there were five Category 5 hurricanes in the
968 CMIP3/A1B ensemble results (0.185 storms per year). The p-levels in parentheses are the
969 estimate probabilities of incorrectly rejecting the null hypothesis of no change in the metric,
970 based on one-sided Mann-Whitney Wilcoxon tests. Two-sided tests were used for translation
971 speed, Hurr (3-5), and Hur (Cat 3) statistics. One-sided tests were used for other metrics; these
972 p-values can be converted to two-sided results by multiplying the p-value by two. Bold
973 highlights changes that are significant at the 0.05 level.
974

975

ZETAC Regional MODEL

VARIABLE	OBS	Means CONTROL	% Change (p-level) CMIP3	CMIP5-EARLY	CMIP5-LATE
Ts (0-5) freq	9.00	11.26	**-27.3 (<0.01)**	**-20.4 (0.02)**	**-22.7 (0.02)**
Hur(1-5) freq	5.30	6.19	-17.4 (0.15)	-5.4 (0.36)	-18.6 (0.08)
PDI	235.33	179.12	**-21.1 (0.04)**	-21.0 (0.05)	**-23.3 (0.03)**
maxwnd_ts	39.44	34.13	3.5 (0.05)	2.4 (0.07)	**2.9 (0.04)**
maxwnd_hur	49.57	38.76	**2.0 (0.05)**	-0.7 (0.14)	**2.2 (0.04)**
landfall_ts	2.37	2.19	-16.9 (0.27)	18.6 (0.10)	3.4 (0.46)
landfall_hurr	1.04	0.96	-23.1 (0.38)	3.8 (0.36)	-11.5 (0.40)
Trans speed	6.64	6.38	2.1 (0.27)	-4.7 (0.03)	-1.9 (0.26)
rain rate ts	-999	185.99	**18.8 (<0.01)**	**7.8 (0.04)**	**13.4 (<0.01)**
rain rate hurr	-999	278.15	**16.7 (<0.01)**	3.1 (0.34)	**9.0 (0.02)**
TS (Cat 0)	3.70	5.1	**-39.4 (<0.01)**	**-38.7 (<0.01)**	**-27.7 (0.02)**
Hurr (Cat 1)	1.89	5.41	**-25.3 (0.05)**	-2.7 (0.46)	-23.3 (0.05)
Hurr (Cat 2)	1.04	0.78	38.1 (0.11)	-23.8 (0.49)	14.3 (0.15)

HURRICANE MODEL DOWNSCALE

VARIABLE	OBS	Means CONTROL	% Change CMIP3	CMIP5-EARLY	CMIP5-LATE
Ts (0-5) freq	9.00	10.85	**-27.0 (<0.01)**	**-22.0 (<0.01)**	**-24.2 (<0.01)**
Hur(1-5) freq	5.30	8.02	**-31.9 (<0.01)**	**-23.1 (<0.01)**	**-28.2 (<0.01)**
Hurr (3-5)	2.37	2.70	-17.1 (0.17)	-6.8 (0.63)	-15.8 (0.25)
Hurr (4-5)	1.37	0.57	**87.1 (0.01)**	45.2 (0.06)	38.7 (0.11)
Hur_ws>65	0.52	0.11	**250.0 (0.05)**	83.3 (0.25)	83.3 (0.17)
PDI	235.33	183.05	**-17.2 (0.04)**	-12.3 (0.09)	**-20.1 (0.02)**
maxwnd_ts	39.44	41.12	0.7 (0.20)	**3.4 (0.04)**	1.7 (0.18)
maxwnd_hur	49.57	46.09	**6.1 (<0.01)**	**4.5 (<0.01)**	**4.0 (0.02)**
Trans speed	6.64	5.57	6.0 (0.22)	-3.0 (0.23)	-2.0 (0.31)
Rain rate_ts	-999	160.88	**22.1 (<0.01)**	**18.2 (<0.01)**	**19.2 (<0.01)**
rain rate_hur	-999	226.17	**22.1 (<0.01)**	**11.4 (<0.01)**	**21.6 (<0.01)**
TS (Cat 0)	3.70	2.83	-13.1 (0.10)	**-19.0 (0.04)**	-13.1 (0.07)
Hur (Cat 1)	1.89	3.41	**-51.6 (<0.01)**	**-41.3 (<0.01)**	**-43.5 (<0.01)**
Hur (Cat 2)	1.04	1.91	-17.5 (0.17)	-13.6 (0.23)	-18.4 (0.10)
Hur (Cat 3)	1.00	2.13	**-45.2 (<0.01)**	-20.9 (0.10)	**-30.4 (0.01)**
Hur (Cat 4)	1.00	0.56	**83.3 (0.01)**	46.7 (0.05)	30.0 (0.21)
Hur (Cat 5)	0.37	0.02	200.0 (0.37)	0. (---)	300.0 (0.31)

976

STATISTICAL REFINEMENT

VARIABLE	OBS	Means CONTROL	% Change CMIP3	CMIP5-EARLY	CMIP5-LATE
Ts (0-5) freq	9.00	11.26	**-27.3 (<0.01)**	**-20.4 (0.02)**	**-22.7 (0.02)**
Hur(1-5) freq	5.3	7.41	**-24.0 (0.04)**	-14.5 (0.15)	-19.0 (0.07)

Hurr (3-5)	2.37	2.89	-10.3 (0.36)	-23.1 (0.15)	-11.5 (0.38)
Hurr (4-5)	1.37	0.78	42.9 (0.10)	-19.0 (0.48)	14.3 (0.15)
Hur_ws>65	0.52	0.15	200.0 (0.07)	-25.0 (0.59)	125.0 (0.22)
PDI	235.33	257.78	-15.6 (0.09)	-19.1 (0.09)	-20.1 (0.07)
maxwnd_ts	39.44	39.81	**6.7 (0.05)**	3.8 (0.08)	5.2 (0.05)
maxwnd_hur	49.57	46.33	**6.2 (0.02)**	1.5 (0.46)	4.1 (0.06)
landfall_ts	2.37	2.18	-17.0 (0.27)	18.6 (0.10)	3.4 (0.46)
landfall_hur	1.04	1.07	-27.6 (0.26)	31.0 (0.12)	-3.4 (0.40)
TS (Cat 0)	3.70	3.85	**-33.7 (<0.01)**	**-31.7 (0.02)**	**-29.8 (0.02)**
Hur (Cat 1)	1.89	2.96	**-37.5 (0.02)**	-20.0 (0.12)	-27.5 (0.08)
Hur (Cat 2)	1.04	1.56	-23.8 (0.19)	11.9 (0.28)	-16.7 (0.26)
Hur (Cat 3)	1.00	2.11	**-29.8 (0.05)**	-24.6 (0.08)	-21.1 (0.10)
Hur (Cat 4)	1.00	0.78	19.0 (0.21)	-19.0 (0.48)	14.3 (0.15)
Hur (Cat 5)	0.37	0.00	*(see caption)	-------	-------

977

978

979

Table 4. As in Table 3, but based on CMIP3-based downscaling experiments for Atlantic tropical storms and hurricanes, using 13 Aug.-Oct. seasons (odd years only from 1981 to 2005) for both control and warm climate conditions. The warm climate experiments use 1981-2005 conditions but with a climate change perturbation (2081-2100 minus 2001-2020) from the CMIP3 18-model ensemble, or from each of ten individual CMIP3 models, added onto the control run conditions. See text for details. The hurricane model results are for the average of runs using the two hurricane model versions (GFDL and GFDN). P-values are not shown, but bold indicates changes that are statistically significant at the 0.05 level, using the tests described in the Table 3 caption..

ZETAC MODEL DOWNSCALING

|---Means----|---------- Percent Changes ----------|

VARIABLE	OBS	Control	CMIP3 ens18	GFDL cm2.1	MPI echam5	Had CM3	MRI cgcm	GFDL cm2.0	Had GEM1	MIROC hi	CCSM3	INGV	MIROC med
TS (Cat 0-5)	8.85	11.08	**-32.6**	-9.0	**-37.5**	**-52.1**	-25.0	7.7	**-61.8**	**-32.6**	-27.8	-22.2	**-43.1**
Hur (Cat 1-5)	5.54	6.38	-24.1	3.6	-34.9	**-57.8**	-14.5	21.7	**-66.3**	-31.3	-12.0	-14.5	**-41.0**
PDI	233.61	177.48	-28.0	4.2	-30.8	**-61.8**	-13.6	20.2	**-68.9**	-27.2	0.8	-19.7	**-43.9**
maxwnd_ts	40.37	34.41	4.0	**4.0**	3.3	-1.9	4.8	**5.4**	-1.9	1.5	**7.5**	3.9	2.1
maxwnd_hur	49.87	38.79	**2.3**	**2.8**	3.6	0.9	4.0	**3.6**	1.5	2.30	3.8	2.0	2.1
Landfall_ts	2.23	2.38	-29.0	0.0	-25.8	-35.5	-38.7	48.4	**-54.8**	-29.0	-12.9	3.2	-35.5
Landfall_hur	1.08	1.54	-45.0	-25.0	-50.0	**-70.0**	**-60.0**	5.0	**-80.0**	-40.0	-30.0	-35.0	-55.0
Trans. Speed	6.40	6.17	3.5	**8.9**	-1.2	4.9	1.4	**11.7**	-0.9	4.5	-2.2	-0.7	-2.6
Rain rate_ts	------	187.24	**20.9**	**22.4**	**23.5**	**12.0**	**28.4**	**26.2**	10.7	**22.3**	**22.5**	**18.5**	**21.5**
Rain rate-hur	------	289.65	**15.3**	**12.5**	**14.2**	2.3	14.5	**14.5**	0.072	5.6	5.7	**9.1**	**13.1**
TS (Cat 0)	3.31	4.69	**-44.3**	-26.2	**-41.0**	**-44.3**	**-39.3**	-11.5	**-55.7**	**-34.4**	**-49.2**	-32.8	**-45.9**
Hur (Cat 1)	1.92	5.38	-27.1	-12.9	-40.0	**-60.0**	-28.6	1.4	**-65.7**	-38.6	-21.4	-15.7	**-47.1**
Hur (Cat 2)	1.00	1.00	-7.7	92.3	-7.7	-46.2	53.8	130.8	-69.2	7.7	38.4	-7.7	-7.7

HURRICANCE MODEL DOWNSCALING:

|---Means----|---------- Percent Changes ----------|

VARIABLE	OBS	Control	CMIP3-ens	GFDL-cm2.1	MPI-echam5	HadCM3	MRI-cgcm	GFDL-cm2.0	HadGEM1	MIROC-hi	CCSM3	INGV	MIROC-med
TS (Cat 0-5)	8.85	10.31	**-28.4**	-4.5	**-32.8**	**-49.3**	-21.6	11.9	**-61.9**	**-34.3**	**-23.1**	**-22.4**	**-42.5**
Hurr (Cat 1-5)	5.54	7.65	**-31.7**	-7.5	**-39.2**	**-61.3**	**-23.6**	14.6	**-70.9**	**-41.2**	-17.1	**-24.1**	**-50.8**
Hurr (Cat 3-5)	2.62	2.54	-18.2	**39.4**	-30.3	**-60.6**	7.6	**71.2**	**-87.9**	**-42.4**	9.1	-1.5	**-39.4**
Hurr (Cat 4-5)	1.46	0.73	73.9	**115.8**	21.1	-52.6	**110.6**	**210.5**	-100.0	-42.1	26.3	47.4	-31.6

Hur (wind>65)	0.62	0.19	220.0	**160.0**	80.0	-60.0	**180.0**	**480.0**	-100.0	20.0	60.0	60.0	20.0
maxwnd_ts	40.37	41.26	3.8	**5.3**	-0.9	-9.2	**6.3**	**9.4**	-10.5	-2.4	7.0	4.8	-3.6
maxwnd_hur	49.87	46.18	**8.2**	**8.6**	**4.2**	2.0	**9.2**	**10.8**	-2.7	2.9	**5.3**	5.9	2.9
Rain rate_ts	-------	162.22	**29.3**	**27.5**	**32.5**	8.2	**23.9**	**34.4**	-4.3	**13.8**	**28.7**	**26.0**	12.0
Rain rate_hur	-------	229.88	**21.9**	**22.4**	**33.1**	7.0	**22.1**	**27.7**	-1.5	11.9	**16.1**	**18.1**	**18.1**
TS (Cat 0)	3.31	2.65	-18.8	4.3	-14.5	-14.5	-15.9	4.3	**-36.2**	-14.5	**-40.6**	-17.4	-18.8
Hurr (Cat 1)	1.92	3.31	**-61.6**	**-39.5**	**-47.7**	**-66.3**	**-45.3**	-30.2	**-75.6**	**-53.5**	**-37.2**	**-40.7**	**-58.1**
Hurr (Cat 2)	1.00	1.81	4.3	-14.9	**-36.2**	**-53.2**	-27.7	17.0	**-38.3**	-17.0	-17.0	-25.5	**-53.2**
Hurr (Cat 3)	1.15	1.81	**-55.3**	8.51	**-51.1**	**-63.8**	-34.0	14.9	**-83.0**	**-42.6**	2.1	-21.3	**-42.6**
Hurr (Cat 4)	1.08	0.69	72.2	**100.0**	16.7	-55.6	72.2	**166.7**	-100.0	-38.9	22.2	44.4	-38.9
Hurr (Cat 5)	0.39	0.04	100.0	400.0	100.0	0.0	800.0	**1000.0**	-100.0	-100.0	100.0	100.0	100.0

995

996

997 **Figure Captions**

998

999 Fig. 1. Means (circles) and ranges (bars) across all simulated years of storm counts for
1000 each model experiment. Filled circles and triangles indicate where the change between
1001 the present day (Control) run and warm climate storm frequency is statistically significant
1002 ($p<0.05$), according to a two-sample, one-sided t-test (filled circle) or a one-sided Mann-
1003 Whitney-Wilcoxon median test (triangles). The sign of the one-sided test used is
1004 indicated by the direction of the triangles. For major hurricanes (c, f), boxes are used
1005 instead of triangles, as two-sided tests were performed for these cases. "Odd Years"
1006 results refer to the 13 (Aug-Oct.) seasons simulated for the individual CMIP3 models.
1007 "All Years" results refer to the 27 (Aug.-Oct.) seasons simulated for the 18-model
1008 ensemble CMIP3 and CMIP5 climate changes. Results were obtained by downscaling
1009 using the Zetac regional model (a-c) or using the Zetac model followed by a second
1010 downscaling step applied to each storm case using the GFDL hurricane model (d-h).
1011 Results are shown for up to five classes of storm intensity: tropical storms and hurricanes
1012 (a, d); hurricanes (b, e); major hurricanes, Category 3-5 (c, f); Category 4-5 hurricanes
1013 (g); and strong Category 4+ hurricanes with maximum winds exceeding 65 m s^{-1} (h).
1014 The GFDL model results (d-h) are based on a two-member ensemble for each case using
1015 two versions of the GFDL hurricane model (GFDL and GFDN). Major hurricanes from
1016 the Zetac model (c) are diagnosed using central pressure rather than maximum winds..

1017

1018 Fig. 2. Comparison of percent changes in frequency of (a) tropical storms and hurricanes
1019 (Category 0-5), and (b) hurricanes (Category 1-5), for the Zetac regional model

experiments vs. the HiRAM C180 global model projections (Aug.-Oct. season) for the late 21st century. Results are shown for the CMIP3/A1B and CMIP5/RCP4.5 multi-model ensembles and for seven common individual model experiments from CMIP3/A1B. The gold lines depict the least squares best fit line through the seven scatterplot points for the seven common individual model experiments.

Fig. 3. Frequency histograms for lifetime maximum surface wind speeds (a, c in m s^{-1}) and minimum surface pressures (b, d in hPa) for observations (black dashed line), control run (thick black), CMIP3/A1B multi-model ensemble (CMIP3-ens18; thick red), and ten CMIP3/A1B individual models (see legend). All results are for the Zetac 18-km grid regional downscaling model (odd years only). Normalized histograms, where the sum of the plotted histogram values is equal to 1 for each curve, are shown in (c, d).

Fig. 4. As in Fig. 3 but for lifetime maximum surface wind speeds from the GFDL hurricane model downscaling experiments (ensemble of GFDL and GFDN versions). Results shown for observations (black dashed line), control run (thick black line), CMIP3/A1B 18-model ensemble (CMIP3-ens18; thick red), and the ten CMIP3/A1B individual models (see legend). Histograms (a) and normalized histograms (b) are shown.

Fig. 5. Scatterplot of projected changes (%) in the mean of the lifetime maximum intensities of all hurricanes for the GFDL and GFDN hurricane model ensemble

(horizontal axis) vs. the statistically adjusted intensities from the Zetac regional model (vertical axis). See legend for identification of experiments.

Fig. 6. As in Fig. 4 but for GFDL hurricane model downscaling experiments based on the CMIP3/A1B and CMIP5/RCP4.5 ensemble mean climate changes. The ensemble of the GFDL and GFDN hurricane model versions are shown, using all 27 years (1980-2006) for the control and perturbed climate samples. Results are shown for the control run (black), CMIP3/A1B 18-model ensemble (CMIP3-ens18; red), CMIP5/RCP4.5 early-21st century ensemble (CMIP5_early; green), and CMIP5/RCP4.5 late-21st century; (CMIP5-late; blue). Histograms (a, b) and normalized histograms (c, d) are shown.

Fig. 7. Tracks and intensities of all storms reaching Category 4 or 5 intensity (>=59 m s^{-1}) in the GFDL hurricane model downscaling experiments (27 seasons), using model versions GFDL (a-d) or GFDN (e-h). Results shown for the control climate (a, e); CMIP3/A1B 18-model ensemble climate change (b, f); CMIP5/RCP4.5 early 21st century ensemble (c, g); and CMIP5/RCP4.5 late 21st century ensemble (d, h).

Fig. 8. Geographical distribution of the projected rate of occurrence (a-d) or change in rate of occurrence (e-h) of Category 4-5 storms for control (a), CMIP3/A1B ensemble (b,e), CMIP5/RCP4.5 early 21st century ensemble (c,f) or CMIP5/RCP4.5 late 21st century ensemble (c,e). The combined results obtained using the GFDL and GFDN

versions of the GFDL hurricane model (scaled as storm occurrences per decade in 10^{o}x10^{o} grid boxes) are shown.

Fig. 9. Changes (warm climate minus control; Aug-Oct. season) in large-scale environmental fields from the original CMIP3 and CMIP5 climate model experiments and time periods (see text). Left column: SST change (color shading) and the "relative SST change field" computed as local SST change minus the tropical mean (30^{o}N-30^{o}S) SST change in Kelvin (contour, with hatching indicating where the SST warming is less than the tropical mean SST warming); middle column: tropical cyclone PI change (m s^{-1}); right column: difference in vertical wind shear vector (200 hPa minus 850 hPa; in m s^{-1}) magnitude between the warm climate and control. Bottom two rows labeled "CMIP3-2xCO2" and "CMIP5-2xCO2" were computed from linear trends over years 1-70 of +1%/yr CO2 experiments using data from the CMIP3 and CMIP5 model archives. Further details of computation methods for SST, PI, and wind shear are given in Vecchi and Soden (2007b).

Fig. 10. (a, b) As in Fig. 1 except for rain rate averaged within 100 km of the storm center and averaged over all tropical storm and hurricane periods [mm day^{-1}] for the Zetac regional model (a) or the GFDL/GFDN hurricane model ensemble (b). (c) Scatterplot (hurricane model vs. Zetac model) of changes [%] between the control and warm climate in hurricane rainfall rate averaged within 100 km of the storm center for the CMIP3/A1B late 21^{st} century ensemble (black) and individual CMIP3 models. The dashed line illustrates a one-to-one relation between the results from the two modeling frameworks.

Fig. 11. Change [%] between the control and warm climate in average hurricane rainfall rate for various averaging radii about the storm center [km] for the CMIP3/A1B (black) and CMIP5/RCP4.5 (red) late 21st century multi-model ensemble climate changes, based on the Zetac regional model (thin solid lines) or the GFDL/GFDN hurricane model ensemble (thick solid lines). The dashed lines illustrate idealized water vapor content scaling, obtained by multiplying the average SST change in the region 10-25^{o}N, 20-80^{o}W by 7% per degree Celsius.

Fig. 12. Comparison of published dynamical-model projections of Atlantic-basin tropical storm frequency changes versus the statistical downscaling model of Villarini *et al*. (2011), which is based on relative SST changes. The figure shows that in most cases where the dynamical models projected increased tropical storm frequency, those models were usually being forced with or had internally computed SST warming of the tropical Atlantic that exceeded the tropical mean. The blue stars depict the CMIP3, CMIP5-Early and CMIP5-Late multi-model ensemble results from the Zetac model.

1108

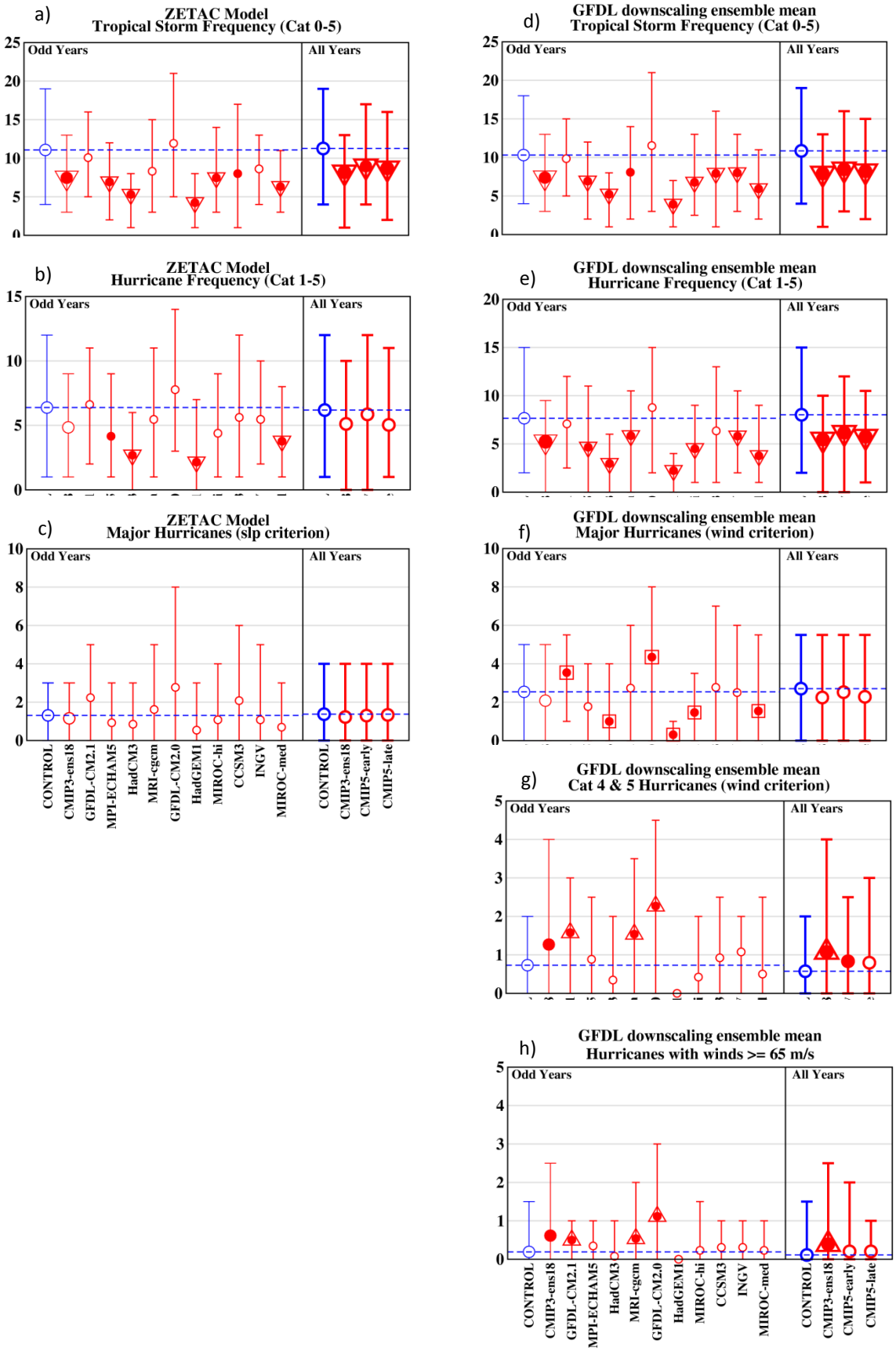
a)
ZETAC Model
Tropical Storm Frequency (Cat 0-5)
Odd Years
All Years
b)
ZETAC Model
Hurricane Frequency (Cat 1-5)
Odd Years
All Years
c)
ZETAC Model
Major Hurricanes (slp criterion)
Odd Years
All Years
CONTROL
CMIP3-ens18
GFDL-CM2.1
MPI-ECHAM5
HadCM3
MRI-cgcm
GFDL-CM2.0
HadGEM1
MIROC-hi
CCSM3
INGV
MIROC-med
CONTROL
CMIP3-ens18
CMIP5-early
CMIP5-late
d)
GFDL downscaling ensemble mean
Tropical Storm Frequency (Cat 0-5)
Odd Years
All Years
e)
GFDL downscaling ensemble mean
Hurricane Frequency (Cat 1-5)
Odd Years
All Years
f)
GFDL downscaling ensemble mean
Major Hurricanes (wind criterion)
Odd Years
All Years
g)
GFDL downscaling ensemble mean
Cat 4 & 5 Hurricanes (wind criterion)
Odd Years
All Years
h)
GFDL downscaling ensemble mean
Hurricanes with winds >= 65 m/s
Odd Years
All Years
CONTROL
CMIP3-ens18
GFDL-CM2.1
MPI-ECHAM5
HadCM3
MRI-cgcm
GFDL-CM2.0
HadGEM1
MIROC-hi
CCSM3
INGV
MIROC-med
CONTROL
CMIP3-ens18
CMIP5-early
CMIP5-late

Fig. 1. Means (circles) and ranges (bars) across all simulated years of storm counts for each model experiment. Filled circles and triangles indicate where the change between the present day (Control) run and warm climate storm frequency is statistically significant ($p<0.05$), according to a two-sample, one-sided t-test (filled circle) or a one-sided Mann-Whitney-Wilcoxon median test (triangles). The sign of the one-sided test used is indicated by the direction of the triangles. For major hurricanes (c,f), boxes are used instead of triangles, as two-sided tests were performed for these cases. "Odd Years" results refer to the 13 (Aug-Oct.) seasons simulated for the individual CMIP3 models. "All Years" results refer to the 27 (Aug.-Oct.) seasons simulated for the 18-model ensemble CMIP3 and CMIP5 climate changes. Results were obtained by downscaling using the Zetac regional model (a-c) or using the Zetac model followed by a second downscaling step applied to each storm case using the GFDL hurricane model (d-h). Results are shown for up to five classes of storm intensity: tropical storms and hurricanes (a,d); hurricanes (b,e); major hurricanes, Category 3-5 (c,f); Category 4-5 hurricanes (g); and strong Category 4+ hurricanes with maximum winds exceeding 65 m s^{-1} (h). The GFDL model results (d-h) are based on a two-member ensemble for each case using two versions of the GFDL hurricane model (GFDL and GFDN). Major hurricanes from the Zetac model (c) are diagnosed using central pressure rather than maximum winds.

1130

1131

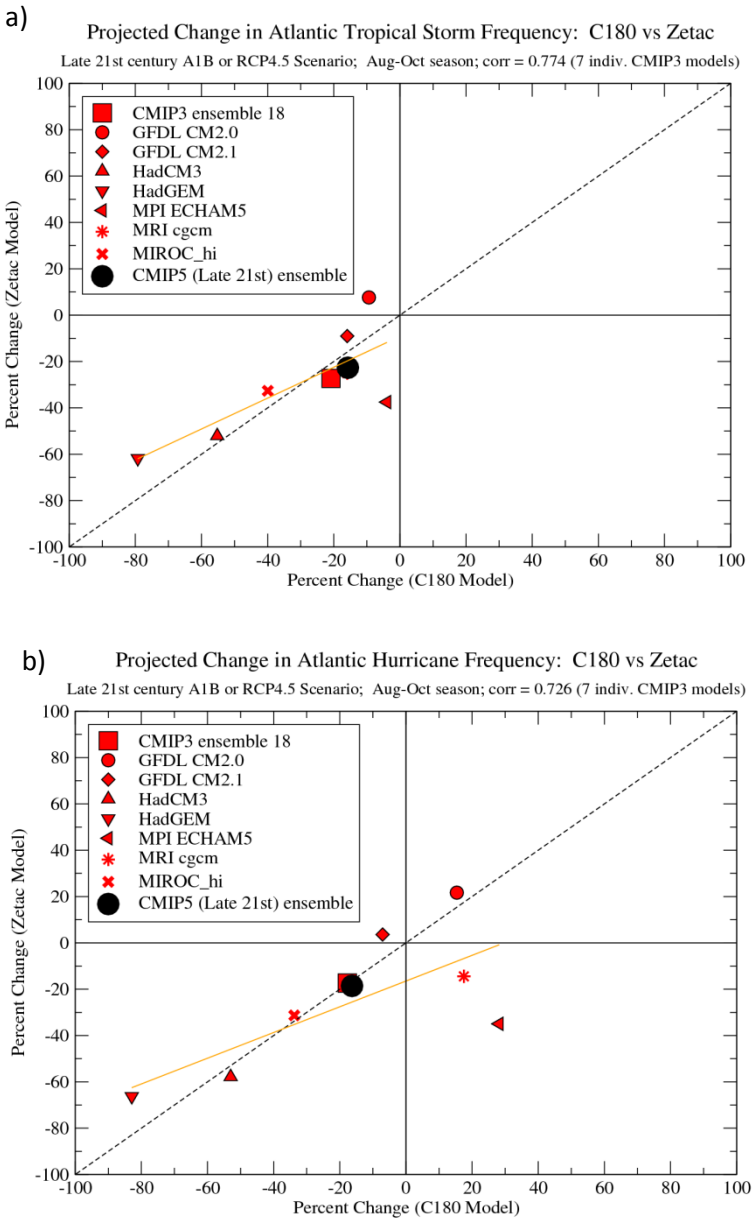

Fig. 2. Comparison of percent changes in frequency of (a) tropical storms and hurricanes (Category 0-5), and (b) hurricanes (Category 1-5), for the Zetac regional model experiments vs. the HiRAM C180 global model projections (Aug.-Oct. season) for the late 21st century. Results are shown for the CMIP3/A1B and CMIP5/RCP4.5 multi-model ensembles and for seven common individual model experiments from CMIP3/A1B. The gold lines depict the least squares best fit line through the seven scatterplot points for the seven common individual model experiments.

1132

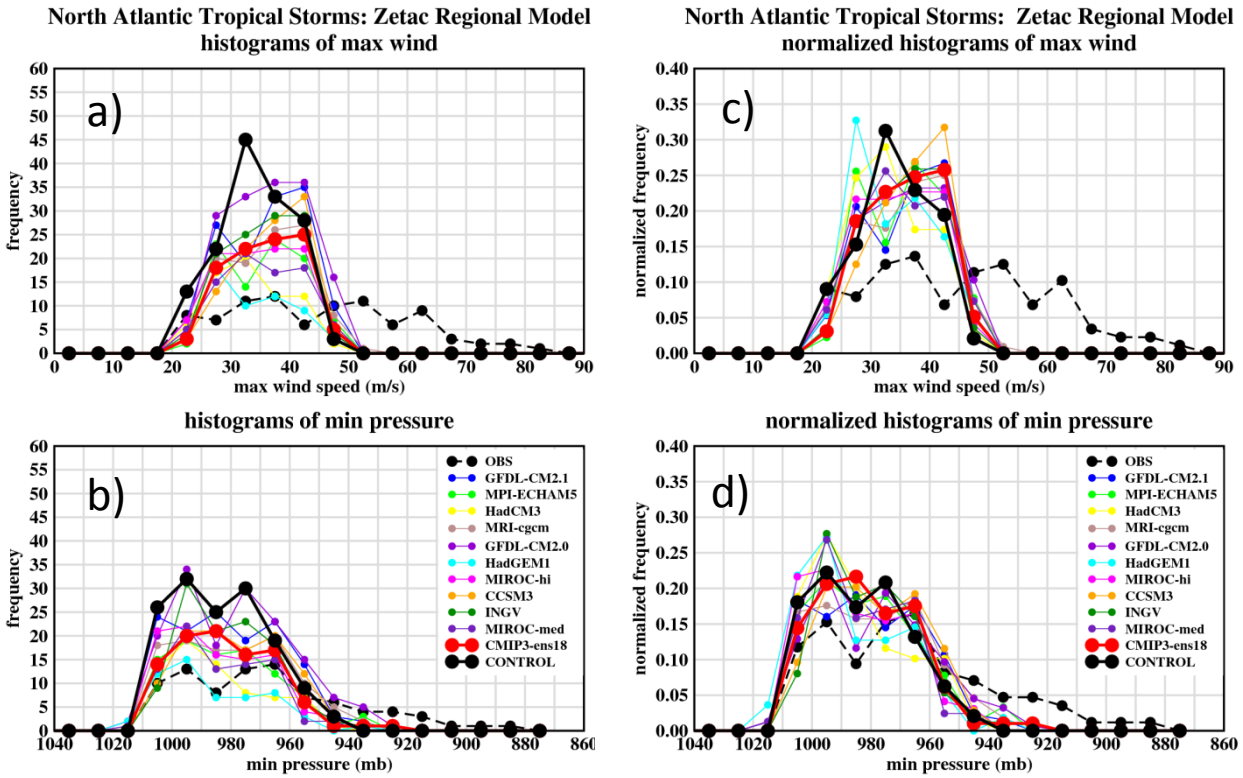

Fig. 3. Frequency histograms for lifetime maximum surface wind speeds (a, c; in m s^{-1}) and minimum surface pressures (b, d; in hPa) for observations (black dashed line), control run (thick black), CMIP3/A1B multi-model ensemble (CMIP3-ens18; thick red), and ten CMIP3/A1B individual models (see legend). All results are for the Zetac 18-km grid regional downscaling model (odd years only). Normalized histograms, where the sum of the plotted histogram values is equal to 1 for each curve, are shown in (c, d).

1133

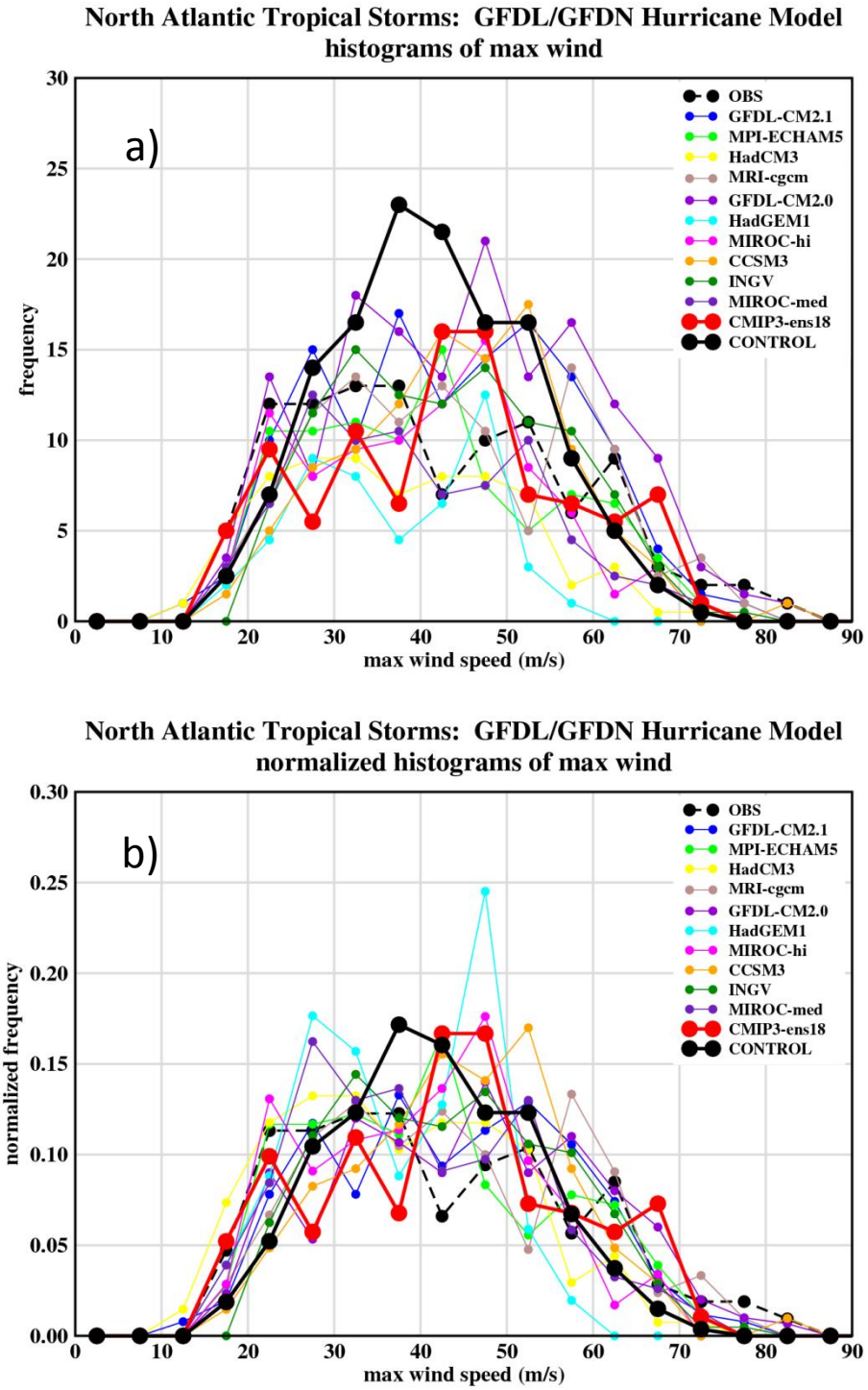

Fig. 4. As in Fig. 3 but for lifetime maximum surface wind speeds from the GFDL hurricane model downscaling experiments (ensemble of GFDL and GFDN versions). Results shown for observations (black dashed line), control run (thick black line), CMIP3/A1B 18-model ensemble (CMIP3-ens18; thick red), and the ten CMIP3/A1B individual models (see legend). Histograms (a) and normalized histograms (b) are shown.

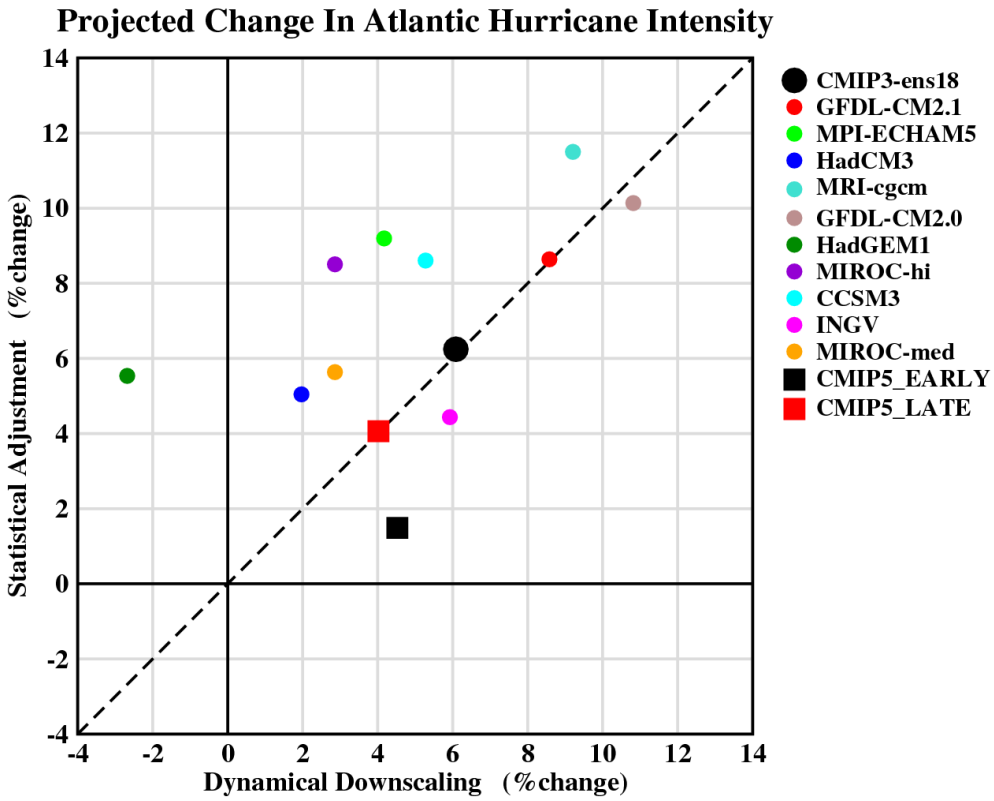

Fig. 5. Scatterplot of projected changes (%) in the mean of the lifetime maximum intensities of all hurricanes for the GFDL and GFDN hurricane model ensemble (horizontal axis) vs. the statistically refined intensities from the Zetac regional model (vertical axis). See legend for identification of experiments.

1141

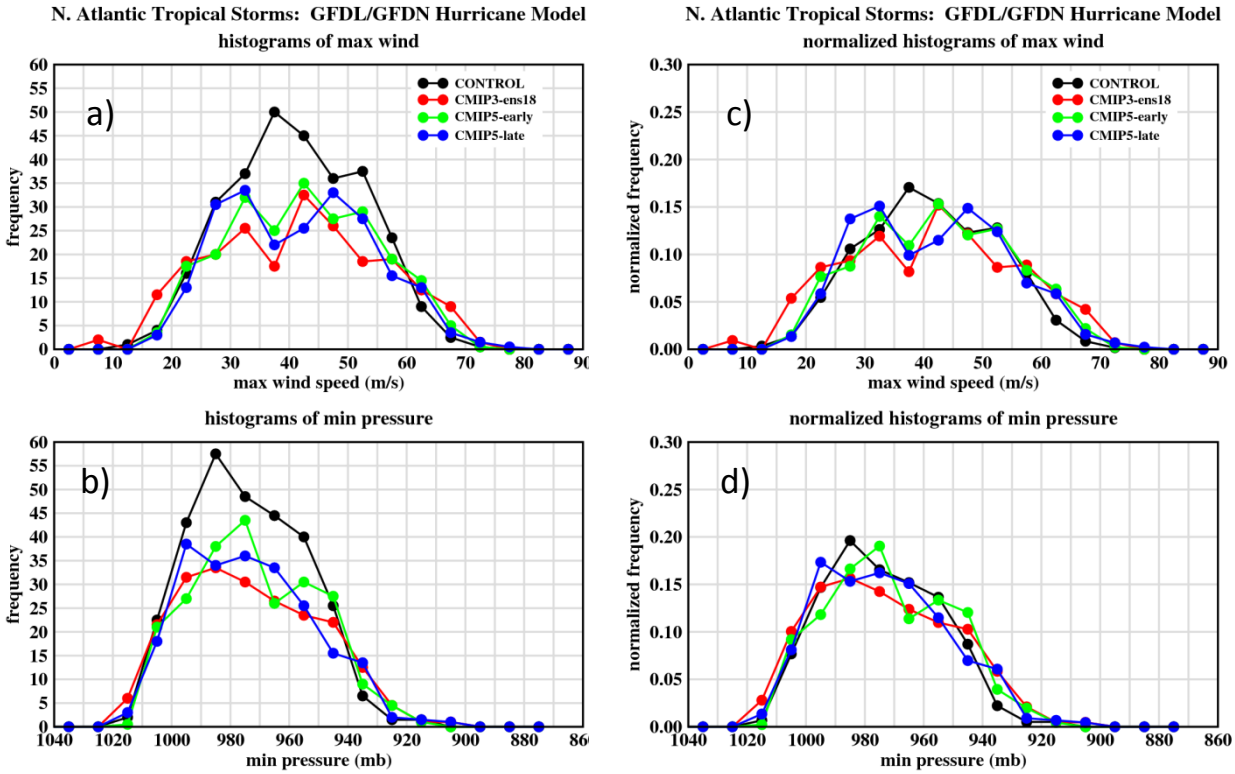

Fig. 6. As in Fig. 4 but for GFDL hurricane model downscaling experiments based on the CMIP3/A1B and CMIP5/RCP4.5 ensemble mean climate changes. The ensemble of the GFDL and GFDN hurricane model versions are shown, using all 27 years (1980-2006) for the control and perturbed climate samples. Results are shown for the control run (black), CMIP3/A1B 18-model ensemble (CMIP3-ens18; red), CMIP5/RCP4.5 early-21st century ensemble (CMIP5_early; green), and CMIP5/RCP4.5 late-21st century; (CMIP5-late; blue). Histograms (a, b) and normalized histograms (c, d) are shown.

1142

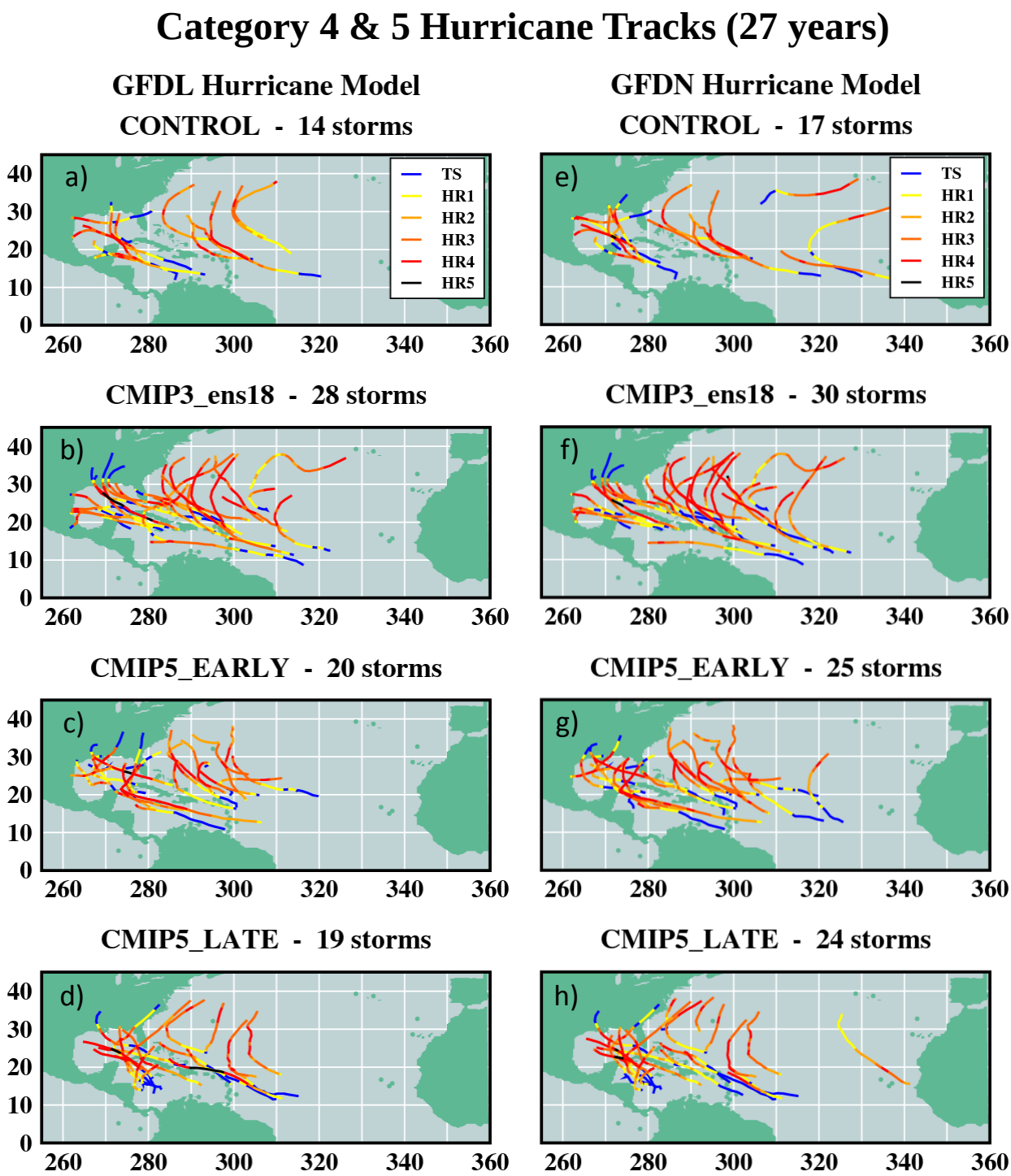

Fig. 7. Tracks and intensities of all storms reaching Category 4 or 5 intensity (>=59 m s^{-1}) in the GFDL hurricane model downscaling experiments (27 seasons), using model versions GFDL (a-d) or GFDN (e-h). Results shown for the control climate (a, e); CMIP3/A1B 18-model ensemble climate change (b, f); CMIP5/RCP4.5 early 21st century ensemble (c, g); and CMIP5/RCP4.5 late 21st century ensemble (d, h).

1143

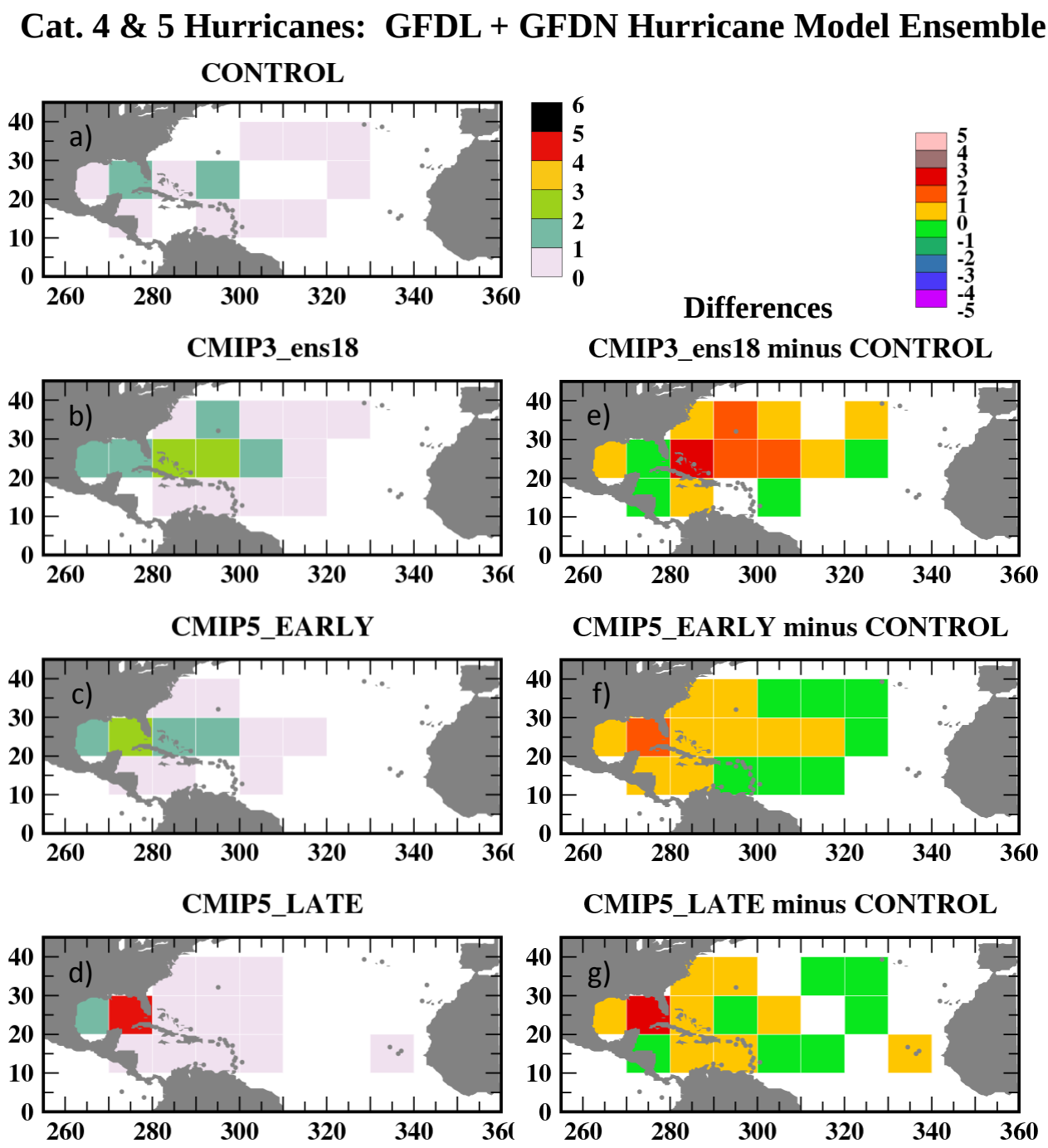

Fig. 8. Geographical distribution of the projected rate of occurrence (a-d) or change in rate of occurrence (e-h) of Category 4-5 storms for control (a), CMIP3/A1B ensemble (b, e), CMIP5/RCP4.5 early 21st century ensemble (c, f) or CMIP5/RCP4.5 late 21st century ensemble (c, e). The combined results obtained using the GFDL and GFDN versions of the GFDL hurricane model (scaled as storm occurrences per decade in 10^{o}x10^{o} grid boxes) are shown.

1144

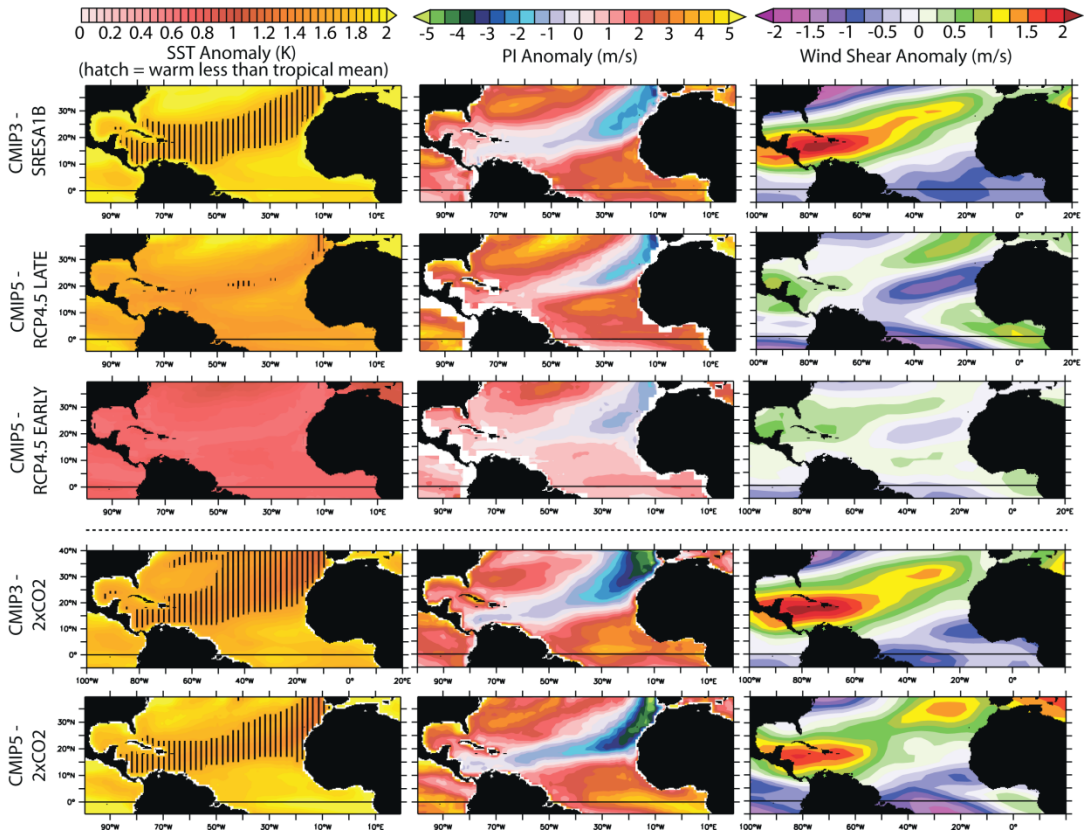

Fig. 9. Changes (warm climate minus control; Aug-Oct. season) in large-scale environmental fields from the original CMIP3 and CMIP5 climate model experiments and time periods (see text). Left column: SST change (color shading) and the "relative SST change field" computed as local SST change minus the tropical mean (30°N-30°S) SST change in Kelvin (contour, with hatching indicating where the SST warming is less than the tropical mean SST warming); middle column: tropical cyclone PI change (m s^{-1}); right column: difference in vertical wind shear vector (200 hPa minus 850 hPa; in m s^{-1}) magnitude between the warm climate and control. Bottom two rows labeled "CMIP3-2xCO2" and "CMIP5-2xCO2" were computed from linear trends over years 1-70 of +1%/yr CO2 experiments using data from the CMIP3 and CMIP5 model archives. Further details of computation methods for SST, PI, and wind shear are given in Vecchi and Soden (2007b).

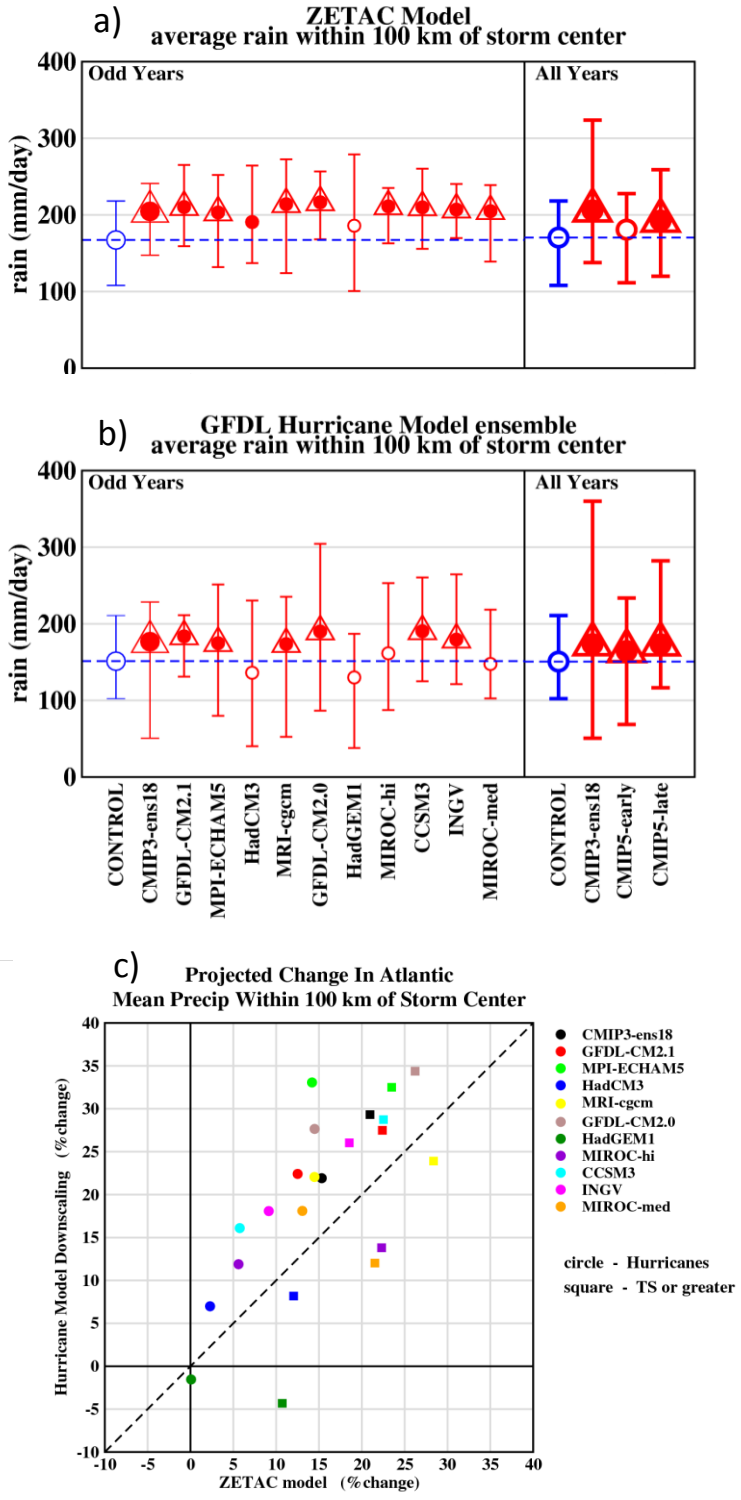

Fig. 10. (a, b) As in Fig. 1 except for rain rate averaged within 100 km of the storm center and averaged over all tropical storm and hurricane periods [mm day^{-1}] for the Zetac regional model (a) or the GFDL/GFDN hurricane model ensemble (b). (c) Scatterplot (hurricane model vs. Zetac model) of changes [%] between the control and warm climate in hurricane rainfall rate averaged within 100 km of the storm center for the CMIP3/A1B late 21st century ensemble (black) and individual CMIP3 models. The dashed line illustrates a one-to-one relation between the results from the two modeling frameworks.

1147

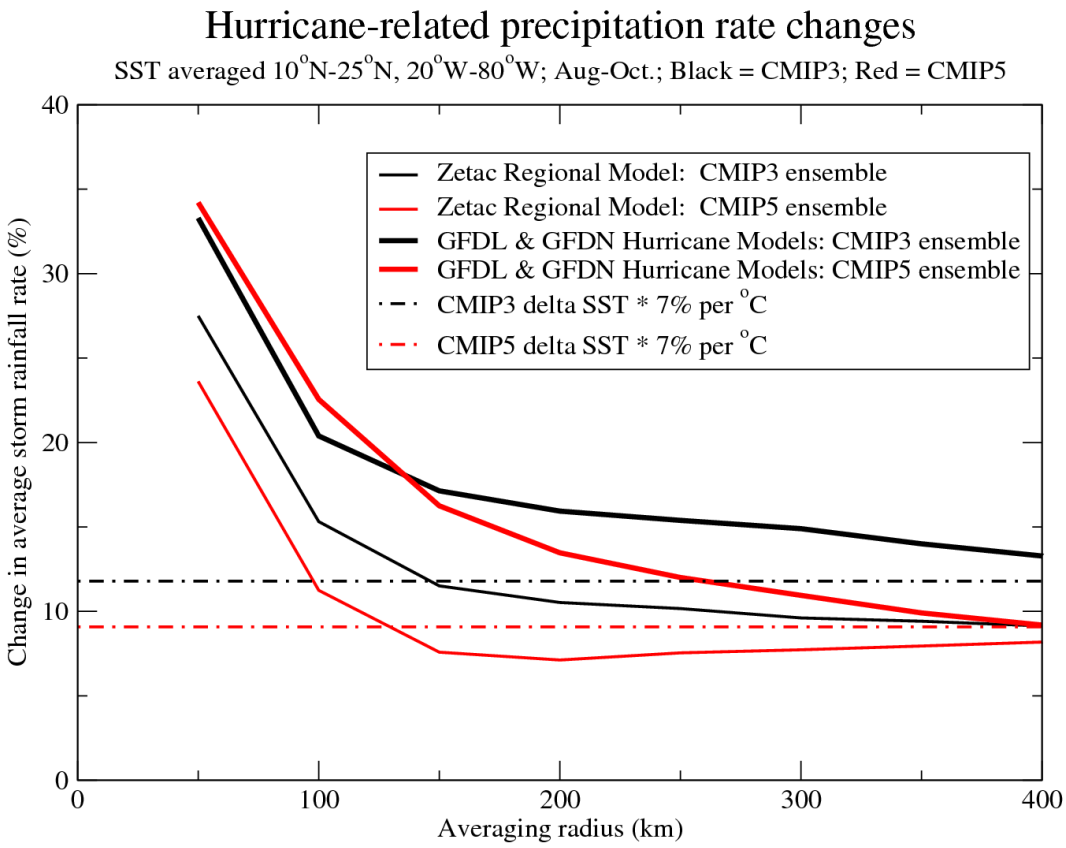

1148

Fig. 11. Change [%] between the control and warm climate in average hurricane rainfall rate for various averaging radii about the storm center [km] for the CMIP3/A1B (black) and CMIP5/RCP4.5 (red) late 21st century multi-model ensemble climate changes, based on the Zetac regional model (thin solid lines) or the GFDL/GFDN hurricane model ensemble (thick solid lines). The dashed lines illustrate idealized water vapor content scaling, obtained by multiplying the average SST change in the region 10-25°N, 20-80°W by 7% per degree Celsius.

1149

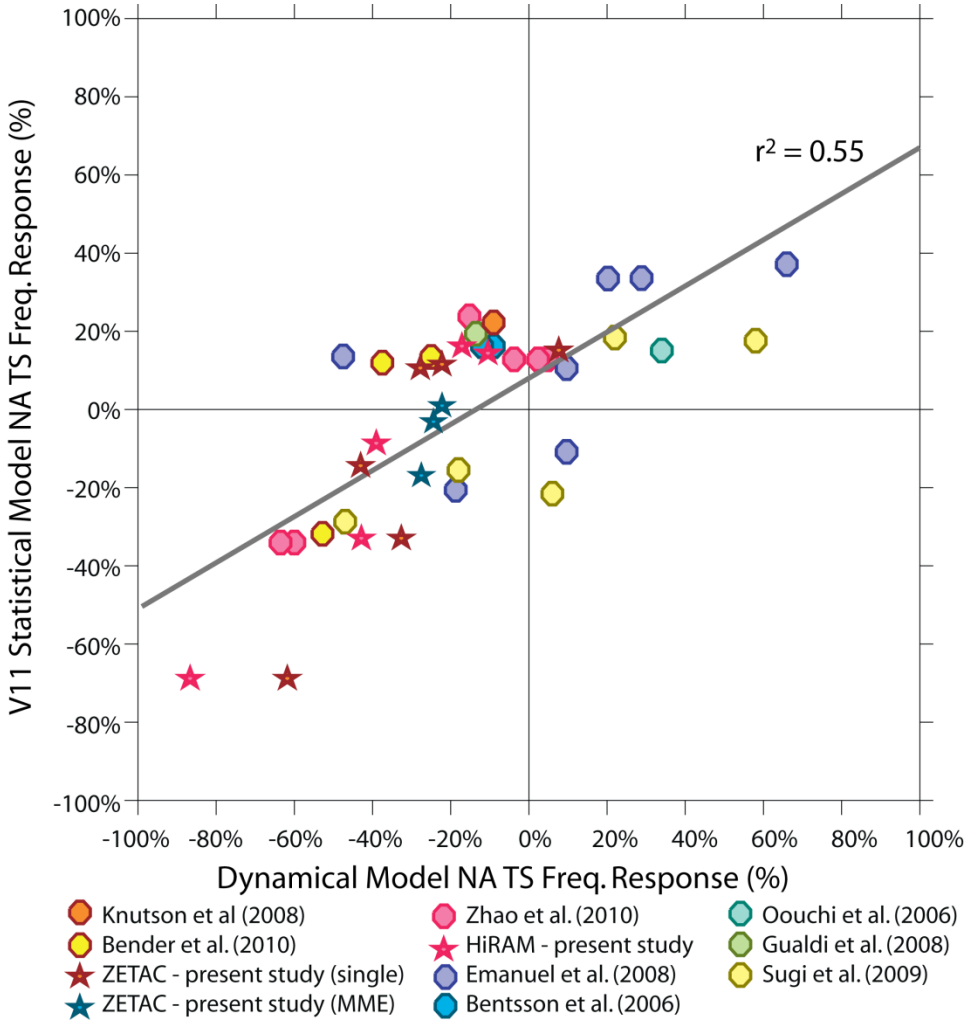

Fig. 12. Comparison of published dynamical-model projections of Atlantic-basin tropical storm frequency changes versus the statistical downscaling model of Villarini *et al*. (2011), which is based on relative SST changes. The figure shows that in most cases where the dynamical models projected increased tropical storm frequency, those models were usually being forced with or had internally computed SST warming of the tropical Atlantic that exceeded the tropical mean. The blue stars depict the CMIP3, CMIP5-Early and CMIP5-Late multi-model ensemble results from the Zetac model.